Probing Inter-Subunit Communication of F_{420} NADP Oxidoreductase: A Kinetic Analysis

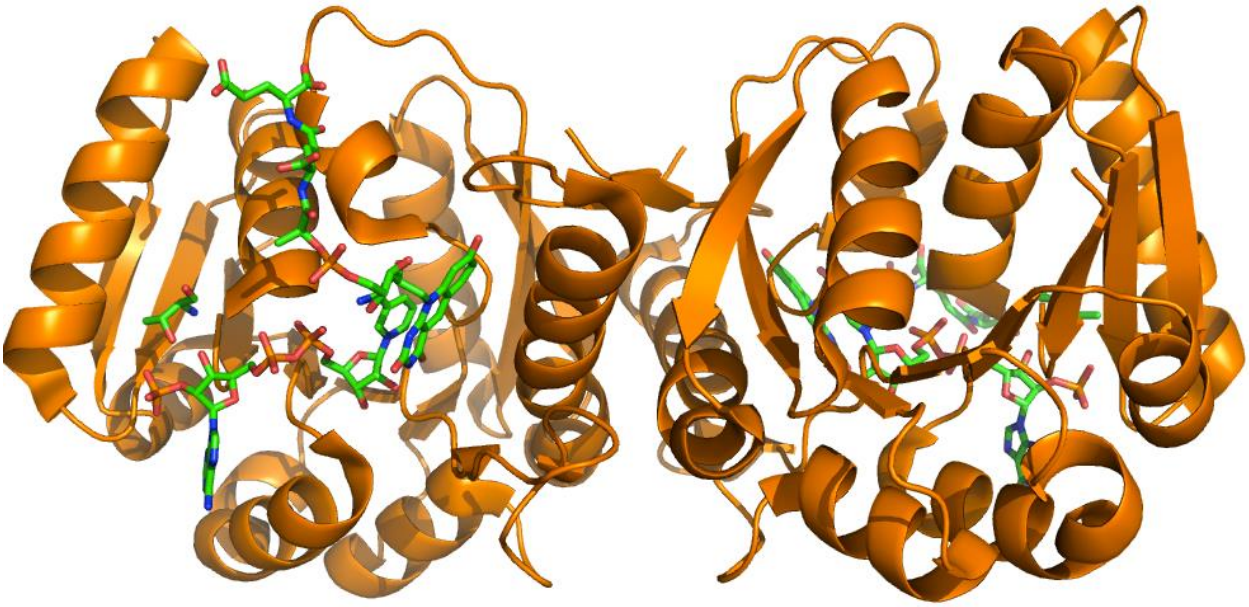

Denzel Pugh

May 2019

Acknowlegements

First, I would like to thank GOD for everything he has done for me. Without the blessings he has bestowed on me I would not be this far or who I am with Him. To my family, you guys were my first teachers, mentors, friends, and people to instill morals and values, while teaching me about the world. You have created a strong foundation for me. One that I still stand on today. One of the many things that you have taught me is to never quit. Also, once you commit, you finish what you start. This is one thing that I have had to keep near and dear to my heart throughout this journey, because at many times I felt lost and questioned my path. So, thanks to my grandparents Marva and Raymond Wandick, my parents Marcus and Sherri Pugh, my brothers Marcus and Jalen, Aunt Teada, Uncle Bill, Uncle Darry , and Uncle O. I will always appreciate the love and support that you have given.

As I think about this experience, I can't help but think about some special teachers and coaches who have helped me along the way. Mrs. Jones, Mr. De'Bose, and Dr. Coleman, words can't express how grateful I am to have elders and mentors in my life like all of you. Each of you have given me lessons to live by and your reach has been with me far past the classroom. Coach Erving and Coach Roberts, you two have been some of the greatest people in my life. I see you as my teachers. The lessons were just different and came outside of the classroom. The two of you, along with Dr. Coleman challenged me in ways that many others haven't. That within itself has been a double-edged sword, because with you I have experienced some of my greatest and worst moments. I couldn't help but reflect on those times because I feel that I have felt similar highs and lows during this graduate school experience. I wouldn't change it for the world, because each of these experiences have been some of the most beneficial and will never leave. I appreciate everyone that I have mentioned thus far because one thing that you all have in common is that you have seen something in me and have always pushed me to be my best, even when I didn't realize you were pushing me to greatness or known what my best could be!

Finally, to my lab mates. I appreciate you all for everything. This is an experience that I will never forget. Lindsay, well Dr. Davis, I wish you all the best! We both have come far from our days at Langston University and as we know, failure is not an option. I know that you will continue to do great things. Just keep fighting and you got it ! Jamariya, I'm so glad that I got to experience this time here with you. I know you are in the beginning, but you are more than capable. Remember, learn not only from my strengths but also my weaknesses! Dr. K, it's so much that I could say, so I'm going to keep it brief. Thanks really doesn't do justice. You have done so much for me that I really don't know how to express my gratitude in words. I know without a doubt, I wouldn't be at this moment without you! I am so appreciative and have to thank God for putting me here and having someone like you ready and in my corner. Thank you for advocating for me and other underrepresented groups. I know that I haven't been the best student however, I hope that you have gained something from me being in your lab, because I have gained so much. Continue to do great works and just know your blessings are coming! Thanks and much love!

Table of Contents

Abstract

F_{420}-dependent enzymes *are important in a number of organisms, which play vital roles in methane production, NADPH regulation, nucleic acid biosynthesis, folate biosynthesis and carbon cycling.* Until our recent publications on F_{420}:$NADP^+$ Oxidoreductase (Fno) and F_{420}-dependent glucose-6-phosphate dehydrogenase **(**FGD), these enzymes, in general, had not been subjected to rigorous enzymological investigation. Our work has provided valuable new mechanistic and functional insights into the enzymes that use this unique cofactor. Our previous kinetic studies on Fno, which is the focus of this proposal, indicated half-site reactivity in only one of the active sites in a functional dimer. These data suggest that Fno participates in negative cooperativity kinetics and that this enzyme regulates NADPH production methanogenic organisms. Based upon our kinetic studies, we have proposed a chemically plausible mechanism and have identified several key amino acids that potentially play an important role in subunit communication within Fno. We are now poised to address three fundamental questions concerning the Fno catalyzed reaction in order to further our understanding of the Fno mechanism. The goal of my project was to investigate the functionality of conserved amino acid residues that are at the interface of the two subunits within Fno. These residues are R186, T192, S190, and H133. To answer this question, we have applied binding studies, steady-state and pre steady-state kinetic methods to assess their kinetic behavior. The data suggests that residues R186 and T192 affect inter-subunit communication. Hydride transfer becomes rate limiting and all of these amino acids are important in catalysis.

List of Illustrations

List of Tables

Introduction

Life has evolved to the use NADH and NADPH as a biological fuel, which transiently stores the reducing equivalents needed to drive numerous essential redox processes. These include the fixation of CO_2 into carbohydrates in photosynthesis, which provides a means to store reducing equivalents for the long term, or into the evolution of methane for organisms needing to dispose of excess reducing equivalents into the environment. Archaea and methanogens are classes of the latter, which as prokaryotes, possess some of the most rudimentary and minimal cellular components required for life. $F_{420}H_2$:$NADP^+$ oxidoreductase (Fno) is an enzyme prevalent in all methane producing organisms (methanogens) and sulfate reducing archaea (1-4). Methanogens play a critical role in carbon cycling, catalyzing the production of methane through the reduction of carbon dioxide. Methanogenic bacteria contain the F_{420} cofactor (Factor 420, (7,8-didemethyl-8-hydroxy-5-deazariboflavin)), which is essential for methanogenesis (methane production). This cofactor is a 5-deazaflavin analog (5) and, like NAD(P), mediates exclusively two-electron transfer reactions (Figure 1). F_{420} cofactor has a favorably low redox potential (-340 to -350 mV), as required for specific energy producing reactions.

The structure of the F_{420} Cofactor is comprised of three six atom fused rings, known as a deazaisoallaxine ring system, along with a ribitol moiety (Figure 1) this is known as FO. Once FO becomes phosphorylated, it is known as F^+. After the addition of the lactyl group the structure is known as F_{420}-0. The addition of the polyglutamate tail can extend from 1-9 times, depending upon the species in which the molecule is found.

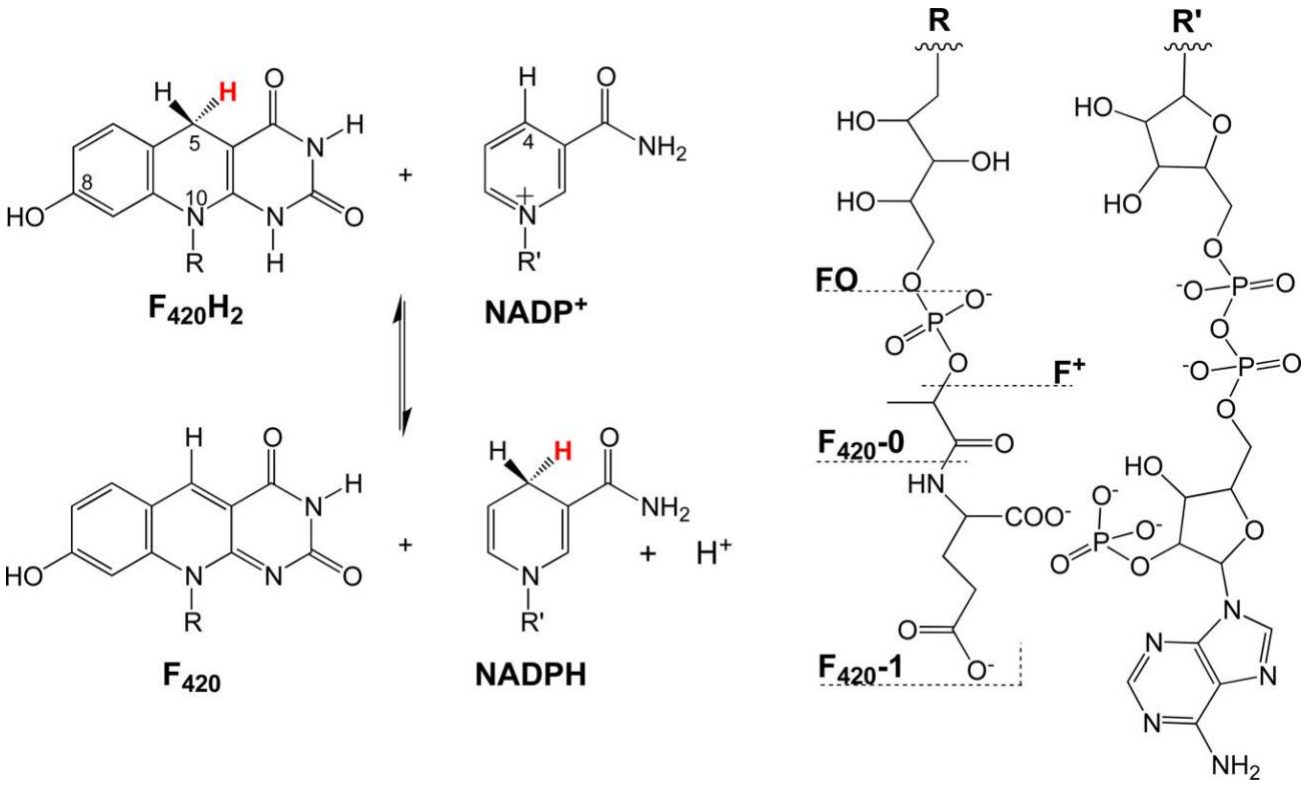

Figure 1. Fno-catalyzed reaction. Fno catalyzes the reversible reduction of NADPH (6) .

In 1972, Cheesman noted that cell free extracts were a dull green color in the presence of nitrogen gas, helium, or air, while they were brown when incubated with hydrogen gas (5). It was later determined that the F_{420} cofactor was largely responsible for this color change. Additionally, 5-deazaflavin compounds are chromophores and are fluorescent by nature. They are fluorescent because of the delocalized electrons in the pi orbitals of the deazaisoalloxazine ring system, which are excited to a pi star state upon exposure to UV – light (7). This particular fluorescent property has been used to identify methanogens (8-14) as well as mycobacterium (15, 16). It is this chemistry that makes the F_{420} cofactor spectrophotometrically distinct (Figure 2).

F_{420} is an obligate two electron molecule, therefore, does not display semiquinone forms, such as the other flavins that have a nitrogen atom in the 5 position. The substitution of the nitrogen in the 5 position to a carbon atom is responsible for the type of chemistry. F_{420} only displays an oxidized form and a reduced form. The oxidized form of the cofactor has a maximum absorbance at 420 nm and the emission spectrum peak

is a maximum at 470 nm (5, 7) . These peaks are pH dependent and at lower pH, the high absorbance peak is shifted to 375 nm and it loses magnitude in the peak's absorbance (5, 7) . Once the oxidized cofactor is reduced, it loses its high absorbance at 420 nm and gains a new smaller peak, a shoulder at 320 nm. This is a key feature which allows us to follow the reduction of the F_{420} cofactor and allows us to kinetically study real time reactions of Fno.

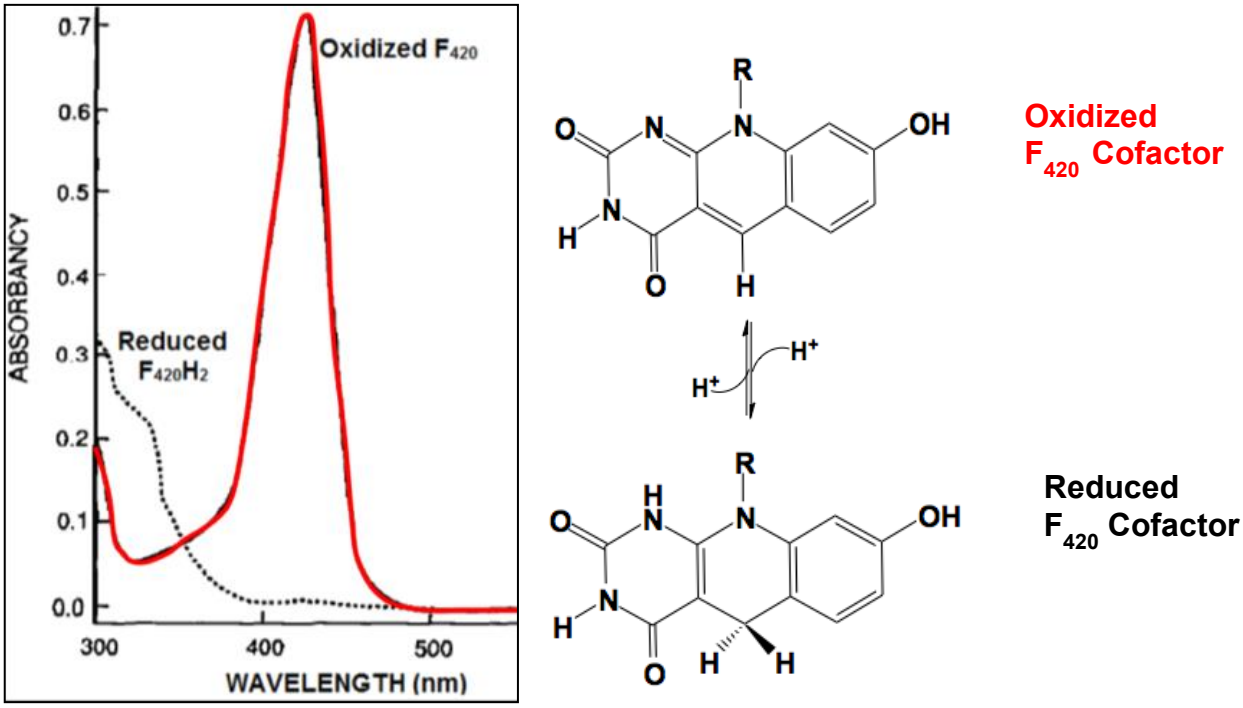

Figure 2: The F_{420} Cofactor Spectrum (17) .

In addition to methanogenic organisms, F_{420} cofactor is found in *Streptomyces, Mycobacteria*, *Nocardia*, methanogenic archaea, sulfate-reducing archaea, and haloarchaea. Because of its high abundance in cells, F_{420} cofactor is believed to be the major electron transfer entity in methanogenic bacteria by transferring electrons from hydrogen atoms to the consecutive intermediates of methane biosynthesis, thereby mediating the bulk of electron flow (5, 17) .

The focus of my thesis is on the methanogenic enzyme, F_{420} NADP Oxidoreductase (Fno). Fno catalyzes a reversible oxidized nicotinamide adenine dinucleotide phosphate ($NADP^+$), using reduced F_{420} cofactor (F_{420}:H_2), which becomes

oxidized in the process (Figure 1) (1) . The crystal structure of Fno has been solved from *Archeoglobus fulgidus and M. thermoautorophicum* (6, 18) . The quanternary structures of each Fno form are different.

The crystal structure of Fno from *A. fulgidus* has revealed that the quanternary structure of Fno is homodimeric with an $\alpha.\beta$ twisted fold (1) . This work by Warkentin *et. al.,* has shown the interface between the monomers are highly hydrophobic. The N-terminal domain (Residues 1 -135) is characterized by two Rossmann folding units arranged as a six stranded beta sheet which surrounded by five alpha helices. The C-terminal domain (Residues 136 – 212) which is much smaller than the N-domain is characterized by two parallel beta strands ($\beta 7 - \beta 8$) and alpha helices ($\alpha\ 7 - \alpha\ 8$).

Fno contains a deep active site pocket between the two domains, which is built up from the small C-terminal segment, $\alpha 8 - \beta\ 9$ and from the loop regions of beta stands 4-6. Due to the proximity of the active site to the dimer interface, it is thought that dimerization is important not only for stability but also for catalysis (1) . Fno is a unique enzyme, structurally it has common architecture similar to that of dinucleotide binding protein family. However, there is no significant sequence similarity (less than 14 percent). The structure was solved with one F_{420} molecule and one $NADP^+$ molecule bound per monomer and revealed that these two cofactors are within 3.1 Å of one another, which is an optimal donor acceptor distance for hydride transfer(1, 19-23) .

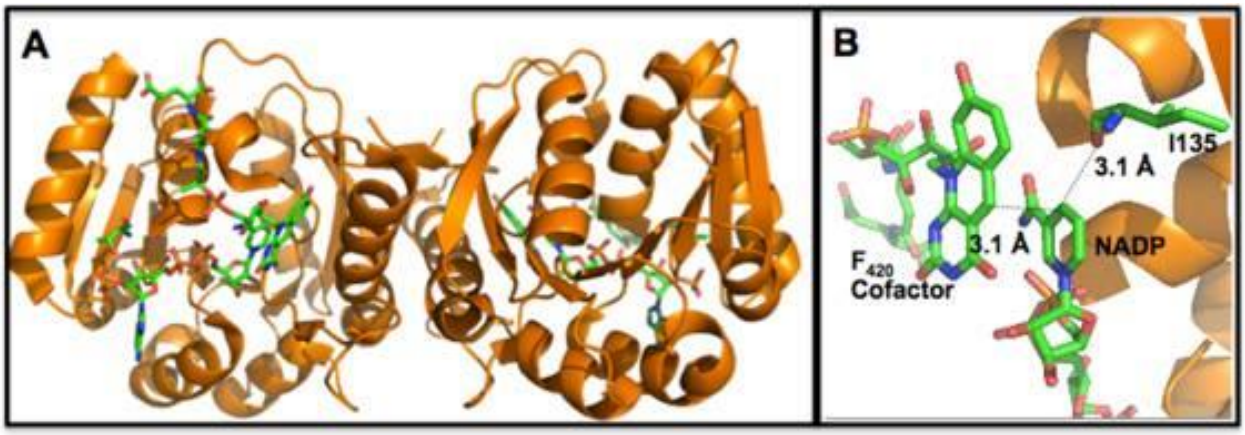

Figure 3 Crystal structure of Fno. A: homodimeric quaternary structure of Fno, in the presence of oxidized F_{420} cofactor and $NADP^+$. B: active site of Fno, PDB file 1jax [1]. The C5 of F_{420} and C4 of $NADP^+$ are 3.1 Å apart, positioned for a direct hydride transfer. I135 is positioned on the $NADP^+$ side, with a 3.1 Å distance from $NADP^+$ within the crystal structure (6) .

The *si*-face of F_{420} faces the nicotinamide ring, while the *re*-face looks toward a hydrophobic wall formed by various side chains (Figure 4) (1). The nicotinamide mononucleotide structure is embedded deep into the active site pocket while the ADP moiety fits into a shallow crevice formed at the C-terminus of beta sheet. Comparing the $NADP^+$ binding with and without a substrate shows an induced conformational change of the enzyme upon NADP binding.

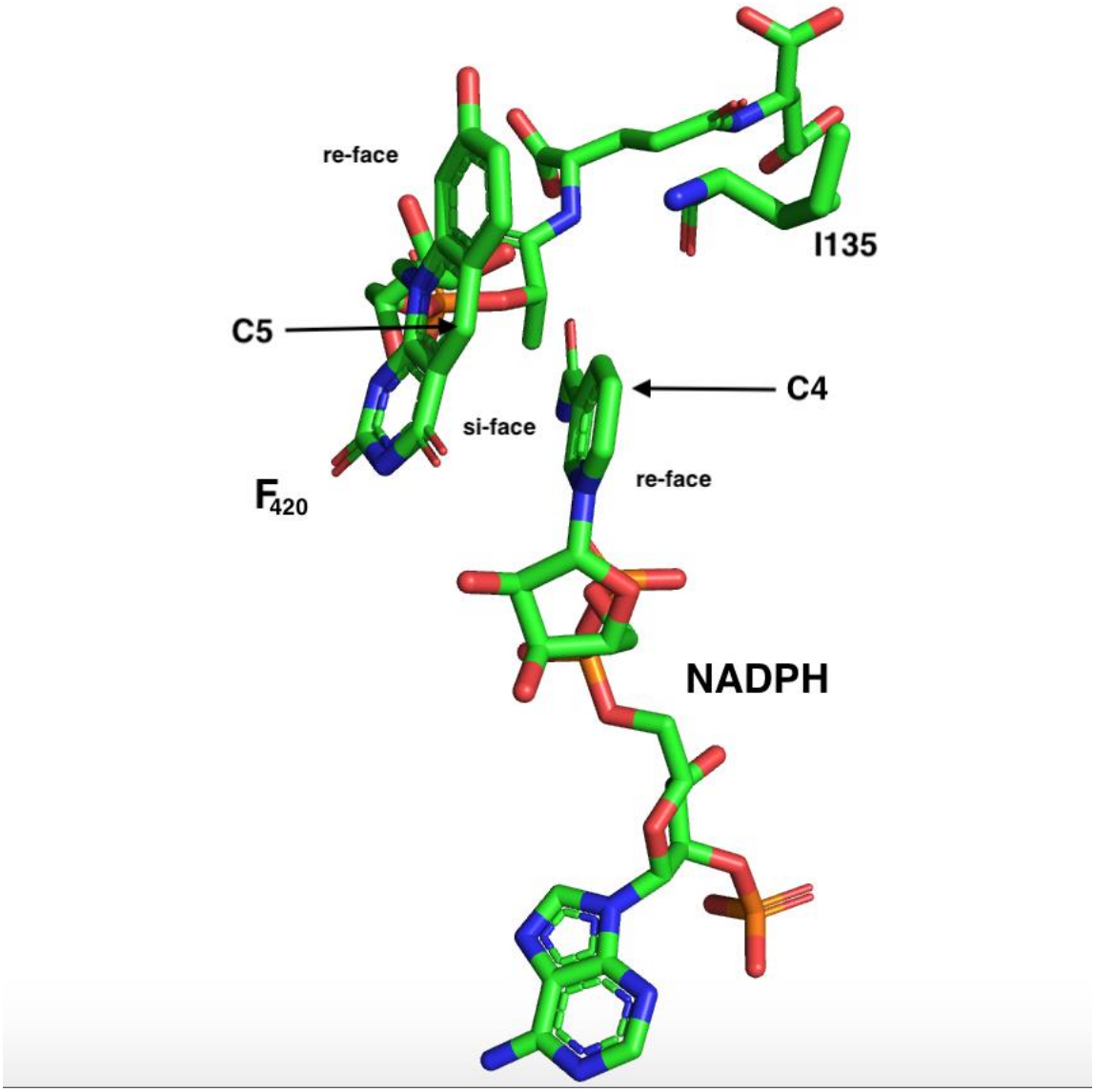

Figure 4 Hydride transfer. The hydride is transferred from the Si-face of F420 towards the Si-face of NADP. The distance between C5 of F_{420} and C4 of NADP is 3.1 A. The proR and proS hydrogen atoms are modelled using the conformation of NADP+ as found in Fno complexed with F_{420} and NADP+, and assuming identical conformations in the oxidized and reduced state. Also shown in dark red is the carbonyl O of Ile135 (1) .

Prior work on Fno from our group reported the first example of half-site reactivity and negative cooperativity within an F_{420} cofactor dependent enzyme. In multi-subunit proteins such as Fno, our steady-state kinetic experiments did not display classical Michaelis-Menten behavior with NADPH was varied at concentrations greater than 100 μM. The double reciprocal plot of the varying NADPH concentrations displays a downward and concave shape, suggesting negative cooperativity between the two identical monomers (Figure 5).

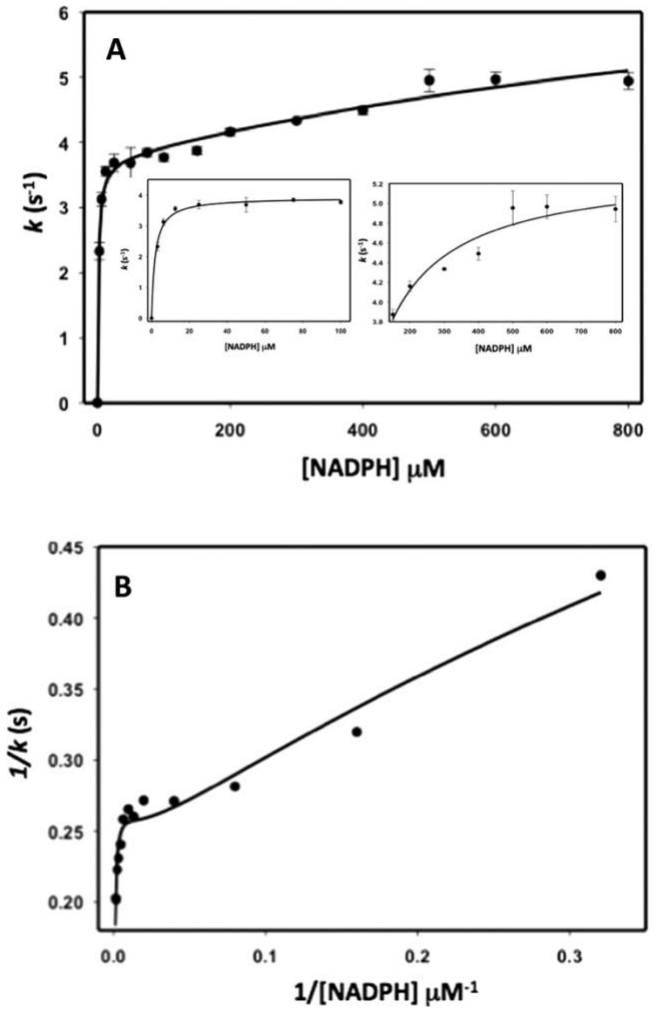

Figure 5. Steady-State Kinetic Behavior of *wt* Fno (6).

We believe that the negative cooperativity kinetics of Fno could be due to a ligand induced conformational changes that affect subunit interactions. Similar observations had been made by Levitizki and Koshland for cytidine triphosphate (CTP) synthetase (3) . Negative cooperativity is explained in detail by a model known as the Koshland-Nemethy-Filmer (KNF) model (24) . In this model the protein is assumed to exist in one confirmation in the absence of a ligand and once a ligand binds to the protein, it causes a conformational change that is transmitted to the other subunit.

Pre steady-state kinetic data shows an initial burst followed by a slow phase (Figure 6). The amplitude of the burst phase correlates to the amount of product produced in only one of the active sites of the dimer. This data indicates that only one subunit of Fno is catalytically active at a time and this type of half site reactivity is referred to as an extreme form of negative cooperativity.

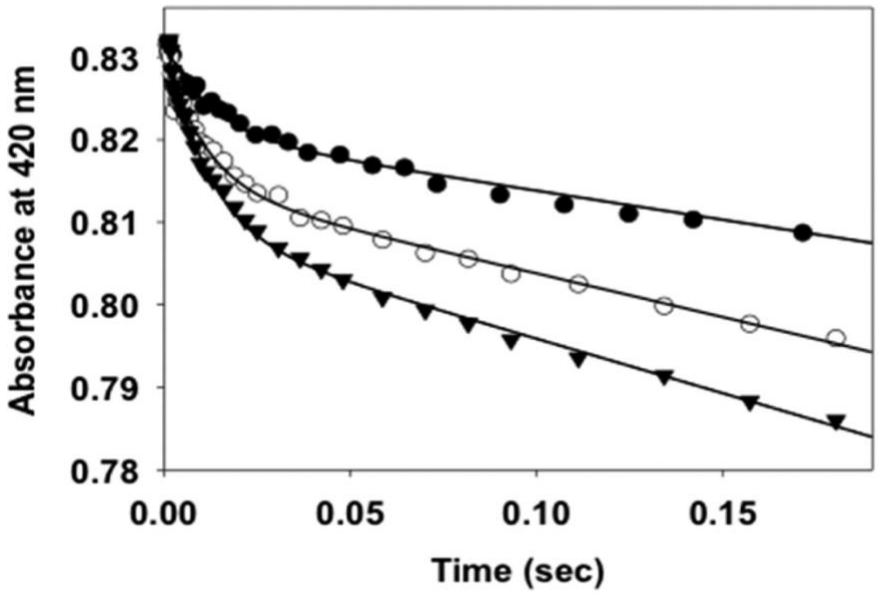

Figure 6. Pre Steady-State Kinetic Behavior of *wt*Fno (6).

Our findings were the first reports in the $F_{420}H_2$:$NADP^+$ oxidoreductases family of enzymes and suggest that Fno is a regulatory enzyme. It is essential within archaea for controlling NADPH concentrations within the cell, which is related to many cellular functions. Based upon the results from our kinetic studies, we proposed a mechanism for Fno (Figure 5). Initially NADPH and FO bind the active site in the subunits for the homodimeric Fno. These binding events causes a conformational change, where the subunits produce an asymmetric dimer, such as when Koshland and Miller described (3). This conformational change makes the second subunit much more difficult to reduce which is negative cooperativity. The hydride transfer occurs in one subunit, which is half site reactivity.

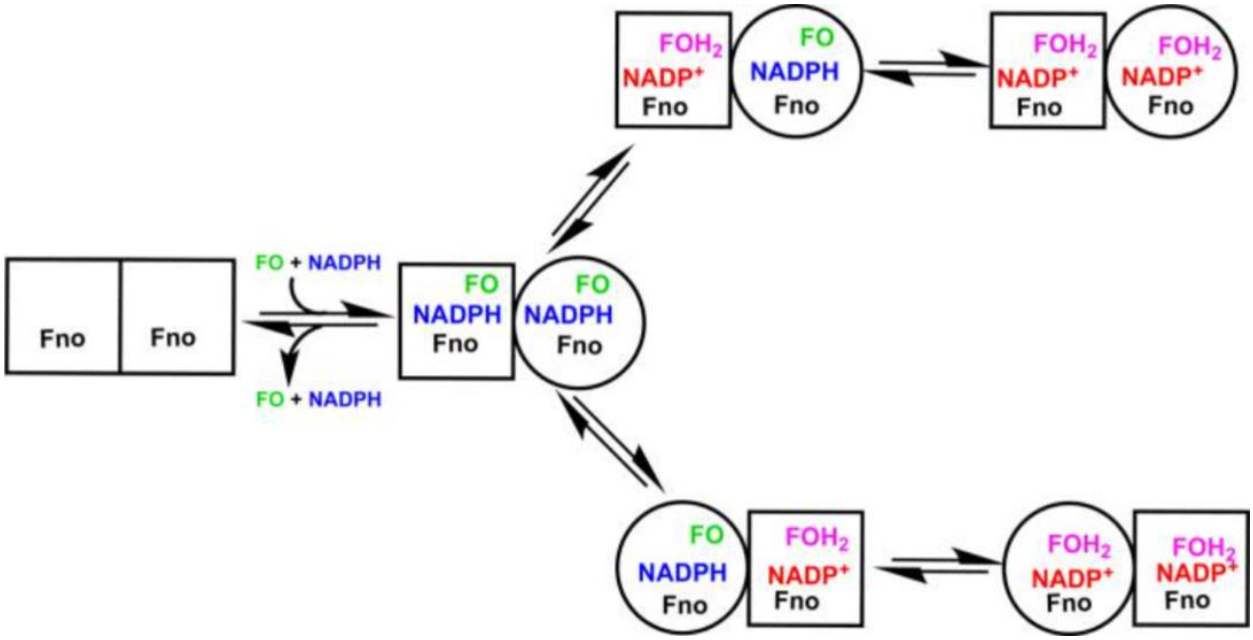

Figure 7. Fno negative cooperativity and half site reactivity and proposed mechanism (6).

To get a more in depth understanding of the possible mechanism of negative cooperativity we took a closer look at the crystal structure.

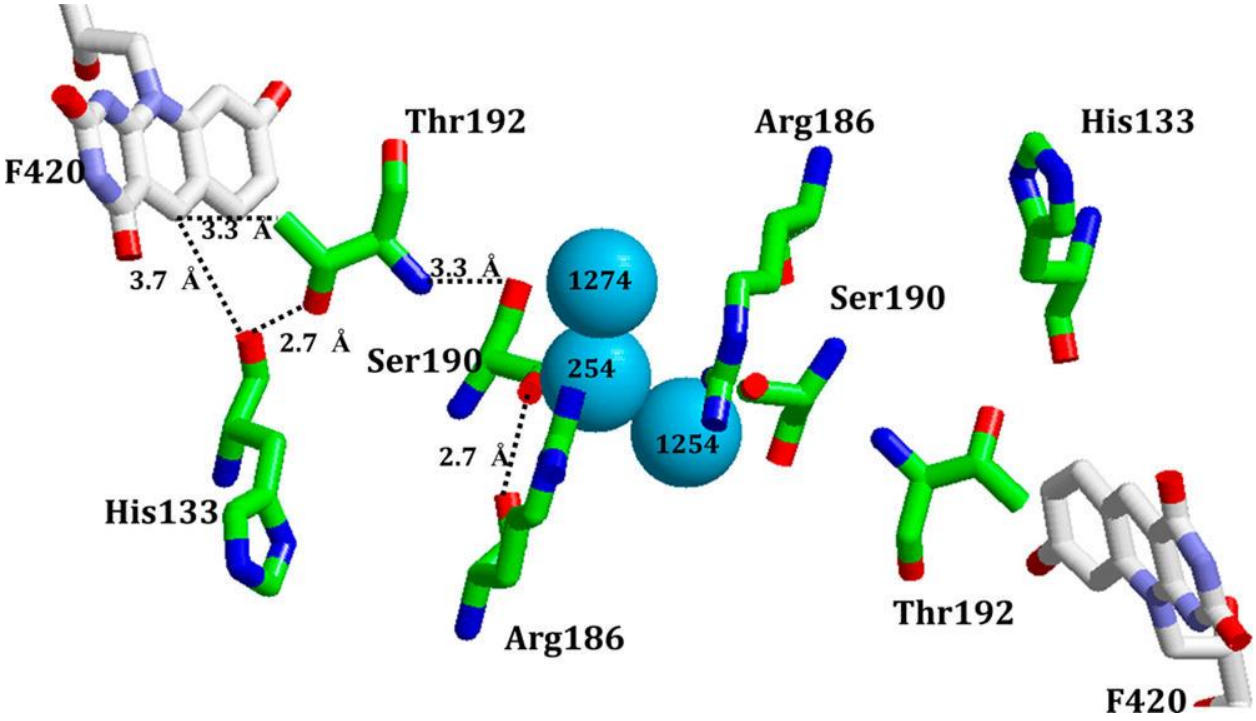

Figure 8. Active Site Connectivity in the Fno Homodimer (6).

Residues H133 and T192 are located close to the carbon in position 5 of the cofactor where the hydride transfer occurs but they don't show any hydrogen bonds with any oxygen or nitrogen with the cofactor (Figure 8). T192 does have a hydrogen bond with the oxygen of S190, which is at the subunit interface between the two domains. The side chain oxygen of S190 forms a Hydrogen bond with another residue on the interface R186. R186 of both subunits could form hydrogen bonds with each other and the side chain oxygens of S190 on each subunit are connected through two water molecules at the interface (Figure 8). We propose that these interactions at the interface provide a basis for inter-subunit communication during catalysis and plays a regulatory role in the negative cooperativity seen in Fno kinetics, which is the basis for my current work. In order to probe the role of these amino acids, we created several Fno variants. Arginine (R) 186 was converted to a lysine (K) in order to probe the charge. Then arginine was converted to a Glutamine (N) and Isoleucine (I) in order to study the polarity.

2.1 Materials and Methods

Reagents

Kanamycin, Tris buffer and ammonium sulfate, Potassium Phosphate dibasic, Potassium Phosphate Monobasic, Luria Broth and MES buffer were all purchased from Fisher Scientific. NADPH was purchased from Sigma Aldrich. The pET24b used for site directed mutagenesis and gene insertion of Fno was purchased from Novagen. Isopropyl β-D-1-thiogalactopyranoside (IPTG) was purchased from Gold Biotechnology. *E. coli* C41(DE3) cells were purchased from Lucigen. Synthesis of FO was reported elsewhere(25) .

Mutagenesis

R186 , T192, H133, Fno primers for the mutagenesis studies area shown in Table 1. Fno gene was cloned into the pET24b by the company Genescript. Site-directed mutations were made in the pET24b using “QuckChange Site-Directed Mutagenesis Kit” from Aglient Technologies. Mutations were confirmed by the company Sequetech Corporation.

Table 1: Primers for Fno variants

Primer	Sequence
R186K Forward	5′ AGT AAT TCC **AAA** CTG GTT GAA 3′
R186K Reverse	5′ TTC AAC CAG **TTT** GGA ATT ACT 3′
R186Q Forward	5′ AGT AAT TCC **CAA** CTG GTT GAA 3
R186Q Reverse	5′ TTC AAC CAG **TTG** GGA ATT ACT 3′
R186I Forward	5′ AGT AAT TCC **ATC** CTG GTT GAA 3′
R186I Reverse	5′ TTC AAC CAG **GAT** GGA ATT ACT 3′
S190A Forward	5′ CTG GTT GAA **GCT** CTG ACG CCG 3′
S190A Reverse	5′ CGG CGT CAG **AGC** TTC AAC CAG 3′
T192V Forward	5′ GAA TCT CTG **GTG** CCG CTG ATT 3′
T192V Reverse	5′ AAT CAG CGG **CAC** CAG AGA TTC 3′
T192A Forward	5′ GAA TCT CTG **GCG** CCG CTG ATT 3′
T192A Reverse	5′ AAT CAG CGG **CGC** CAG AGA TTC 3′
H133A Forward	5′ TCT GCC CTG **GCC** ACG ATC CCG 3′
H133A Reverse	5′ CGG GAT CGT **GGC** CAG GGC AGA 3′
H133N Forward	5′ TCT GCC CTG **AAC** ACG ATC CCG 3′
H133N Reverse	5′ CGG GAT CGT **GTT** CAG GGC AGA 3′

Expression and Purification

Transformation of the mutated Fno plasmids into C41(*DE3*) *E. coli* cells was executed following the protocol by Lucigen Technologies. The muted plasmids were then used for expression. Expression and purification was performed in a similar manner as reported by our lab in prior works (6, 26) with minor changes. Briefly, frozen C41 *DE3* cells containing the Fno gene in the mutated pET24b plasmid was inoculated in 10 L of LB culture with 50 μg/mL of kanamycin at 37 °C until an Optical Density of 1.0 was reached. This culture was then induced with 1 mM IPTG overnight immediately followed by harvesting of cells. Harvested cells were resuspended in 1.5 M potassium phosphate buffer, pH 8.0. Cells were lysed by sonication at 4 °C and centrifuged at 8500 rpm for 30 min at °C. Fno was further purified by heat precipitation at 90 °C for 30 min and the centrifuged again at 8500 rpm for 30 min. Following Heat perception two ammonium sulfate fractionation steps occurred (0 – 40% and the 40 -70%) at 4 °C. Next, Polyethyleneimine (PEI) precipitation, and anion exchange chromatography, using a

DEAE52- Cellulose column were used to purify Fno even further. Finally, a S-200 Sephacryl HR Size Exclusion column (GE Healthcare) was used to desalt the Fno sample. Each of these steps listed after heat precipitation were all followed by centrifugation at 8500 rpm for 20 min at 4 °C.

Binding of FO and NADPH Fno variants

The binding of NADPH and FO experiments have been previously reported for *wt*Fno (6). These experiments for the FNO variants were conducted in similar way as with *wt*Fno with minor changes as described here. Binding experiments were performed using a Horiba Fluoro Max Spectrofluorometer and each individual binding assay were observed in a 160 μl Spectrosil Quartz sub-micro cell from Starna Cells. Every sample was excited at 290 nm and the emission scans were monitored between 300 – 500 nm looking at a decrease in tryptone fan emission at 340 nm. Excitation and emission slit widths were 4 and 8nm. To obtain the K_d (Dissociation Constant) of NADPH, 1 μl aliquots of various concentrations of NADPH (0 – 1780 nM) was titrated with 0.2 μM Fno in 50 mM MES/NaOH at pH 6.5.

To obtain the K_d of FO, various concentration of FO (0-300 nM) were titrated in 0.2 μM of Fno in 50 mM MES/NaOH at pH 6.5. The binding was observed in the same manner as described above for the NADPH binding studies. The decrease in tryptophan emission at 340 nm were used for the calculation of the dissociation constant for both FO and NADPH.

Hill coefficient and dissociation constants for both NADPH and FO binding were determined by fitting the data to a sigmoidal function (Eq. 1) using Sigma Plot version 13.0.

$$\Delta F = [F_{max}\,[L]^n/(K + [L]^n)] \qquad \text{(Eq. 1)}$$

Where, ΔF is equal to the change in fluorescence emission at 340 nm which is caused by the addition of either NADPH or FO as the ligand (L). F_{max} is the normalized maximum fluorescence (F_{max} = 1). To obtain the fractional saturation each normalized

data point was divided by the F_{max}. Hill coefficient is represented by (n) and the dissociation constant is represented by (K_d).

Steady-state kinetics of Fno variants

The steady-state kinetic measurements were carried out using a Cary 100 Bio UV-Vis Spectrophotometer at room temperature (22 °C). To determine the FO steady-state kinetic parameters, a sample of 0.2 μM FNO was mixed with various concentrations of FO (1.3 – 30 μM) and constant 600 μM NADPH in 50 mM MES/NaOH, pH 6.5. To determine the NADPH kinetic parameters, 0.2 μM FNO was mixed with varying concentrations of NADPH (2–1700 μM) in 50 mM MES/ NaOH, pH 6.5 and FO at a constant concentration of 25 μM. The initial rate of each reaction was calculated following the reduction of FO at 420 nm and the data was fit to the Michaelis-Menten equation

$$k = k_{cat}[S]/(K_m + [S]) \qquad \text{(Eq.2)}$$

Pre steady-state kinetics of Fno variants

Rapid kinetic experiments of FNO variants were performed similar to our prior studies with *wt*Fno conductuded by Joseph *et. al*. A sample of 1.0 μM FNO and 10 μM NADPH in 50 mM MES/ NaOH at pH 6.5 was mixed against a constant concentration of 25 μM in 50 mM MES/NaOH at pH 6.5, using a Hitech Scientific DX2 stopped-flow spectrophotometer at 22 °C in diode array mode between 350 – 800 nm. These multiple turnover experiments were repeated using 1.5 μM Fno and also 2.0 μM Fno for each Fno variant. In each of these experiments the reduction of FO, was followed at 420 nm. This data was plotted to determine the pre steady-state parameters using SigmaPlot version 13.0 and fit to the following equation,

$$\text{Absorbance} = A_0 e^{(-kt)} - (vt) + c \qquad \text{(Eq. 3)}$$

where A_0 is the amplitude of the burst phase, *k* is the observed burst rate constant, and *v* is the observed steady-state rate.

2.2 Results

Binding

*wt*Fno has a $^{NADPH}K_d$, of 2.0 ± 0.3 nM, while $^{FO}K_d$ is 3.6 ± 0.7 nM. A K_d of 100 μM or less suggests tight binding or high affinity for substrate to the enzyme. Therefore, Fno has a high affinity for both substrates. The Fno R186 variants (R186K, R186Q, R186I) have dissociation constants for FO, ranging from 3.3 to 6.8 nm (Table 2), meaning that they only effect FO binding minimally because they are in the same range as *wt*Fno. However, these variants have a significant effect (10x or greater) on the enzyme's affinity towards NADPH. The R186K Fno variant changed a large positive charge of the guaninidium group to a point charge within lysine. The binding data reveals that this charge had a large effect on NADPH binding revealing a $^{NADPH}K_d$ of 26 ± 5 μM (Table 2). When the arginine was converted to a glutamine, which completely deleted any positive charge, but preserved the polarity, the binding constant was similar to the R186K Fno variant. However, once the polarity was removed by the conversion of arginine to an isoleucine, there was a two fold increase (46 ± 7μM) in the dissociation constant in comparison to the other arginine variants. This suggests that polarity also plays a significant role in NADPH binding as well (Table 2). The binding data suggests that the other amino acids, T192, S190 and H133 also play a role in NADPH binding, with little to no effect on FO binding (Table 2).

Our previous work on *wt*Fno suggest that the enzyme is regulatory because it displays negative cooperativity kinetics (6). The Hill Coefficient for *wt*Fno is less than 1 (0.61 ± 0.03), which suggest negative cooperativity binding. However, the Hill Coefficients of the R186K, R186Q, T192A, T192V and H133N all are 1 within error (Table 2). This data suggest that we have changed cooperativity binding and the ability of the subunits to communicate effectively.

Table 2: Dissociation constants (K_d) for *wt*Fno and Fno variants

Dissociation constants and Hill coefficients of FO and NADPH for *wt*Fno and variants. The binding studies were carried out in 50 mM MES/NaOH buffer (pH 6.50) at 22 °C in a Horiba FluoroMax Spectrofluorometer. FO or NADPH was titrated into 0.2 µM Fno and the fluorescence emission was monitored at 340 nm after excitation at 290 nm.

Enzyme	$^{NADPH}K_D$ (nM)	NADPH Hill Coefficient	$^{FO}K_D$ (nM)
[a] *wt*Fno	2.0 ± 0.3	0.61 ± 0.03	3.6 ± 0.7
R186K	26 ± 5	0.9 ± 0.1	3.3 ± 0.8
R186Q	19 ± 4	0.8 ± 0.2	6.5 ± 0.4
R186I	46 ± 7	0.7 ± 0.1	6.8 ± 0.9
T192A	22 ± 5	0.8 ± 0.2	5.9 ± 0.6
T192V	26 ± 5	0.9 ± 0.2	4.8 ± 0.4
S190A	27 ± 8	0.7 ± 0.1	12 ± 5
H133N	35 ± 6	1.1 ± 0.2	9 ± 3

Steady-state Kinetics

The steady-state kinetic analysis of *wt*Fno was conducted previously and published (6). The data revealed classical Michaelis-Menten kinetics with varying FO concentrations. However, with varying concentrations of NADPH, the data was biphasic with no saturation out to 1 mM NADPH. The k_{cat} for *wt*Fno was 5.41 ± 0.04 s^{-1}. *wt*Fno is significantly faster than the k_{cat} values for the R186 variants. However the $k_{cat's}$ for the R186 Fno variants ranged from 0.6 – 1.5 s^{-1}. The results are similar for the T192 variants. This suggests that these amino acids are important in catalysis. While *wt*Fno displays biphasic kinetics, these variants do not display a fast and a slow phase (see appendix). These Fno variants require higher concentrations of FO. However, these concentrations are beyond the scope of our instrument. All of the steady state FO plots are affected by this, with the R186Q Fno mutation being the most affected.

Table 3: Steady-State Kinetic Parameters for *wt*Fno and variants

FO steady-state kinetics parameters for *wt*Fno and variants. The steady-state kinetic measurements were carried out using a Cary 100 Bio UV-Vis Spectrophotometer at room temperature (22 °C). A solution of 0.2 µM Fno and 600 µM NADPH in 50 mM MES/NaOH at pH 6.5 was mixed with varying FO concentrations (1.3 µM to 30 µM).

Enzyme	$^{NADPH}k_{cat}$ (s^{-1})	$^{NADPH}K_m$ (µM)	$^{NADPH}k_{cat}/K_m$ (M^{-1} s^{-1})	$^{FO}k_{cat}$ (s^{-1})	$^{FO}K_m$ (µM)	$^{FO}k_{cat}/K_m$ (M^{-1} s^{-1})
[a] *wt*Fno	5.41 ± 0.04 4.16 ± 0.07	2.3 ± 0.2 61 ± 6	2.4×10^6 6.8×10^4	5.3 ± 0.1	4.0 ± 0.4	1.3×10^6
R186K	1.5 ± 0.1	258 ± 30	9.5×10^4	0.78 ± 0.02	8 ± 1	5.8×10^3
R186Q	0.6 ± 0.1	72 ± 7	7.2×10^4	2.1 ± 0.2	29 ± 6	8.3×10^3
R186I	0.87 ± 0.04	65 ± 8	1.3×10^5	1.35 ± 0.04	11 ± 2	1.5×10^4
T192A	0.8 ± 0.1	227 ± 54	1.9×10^5	1.15 ± 0.04	6 ± 1	3.3×10^3
T192V	0.012 ± 0.001	140 ± 34	8.5×10^1	0.040 ± 0.001	11 ± 1	8.5×10^1

Furthermore, when the steady-state date for the R186 Fno variants are displayed as double-reciprocal plots, the data conform to a straight line, suggesting no cooperativity kinetics (Figure 9). This is different than what we see for *wt*Fno which is indicative of negative cooperativity kinetics with a shape that is downward and concave in curvature (Figure 5).

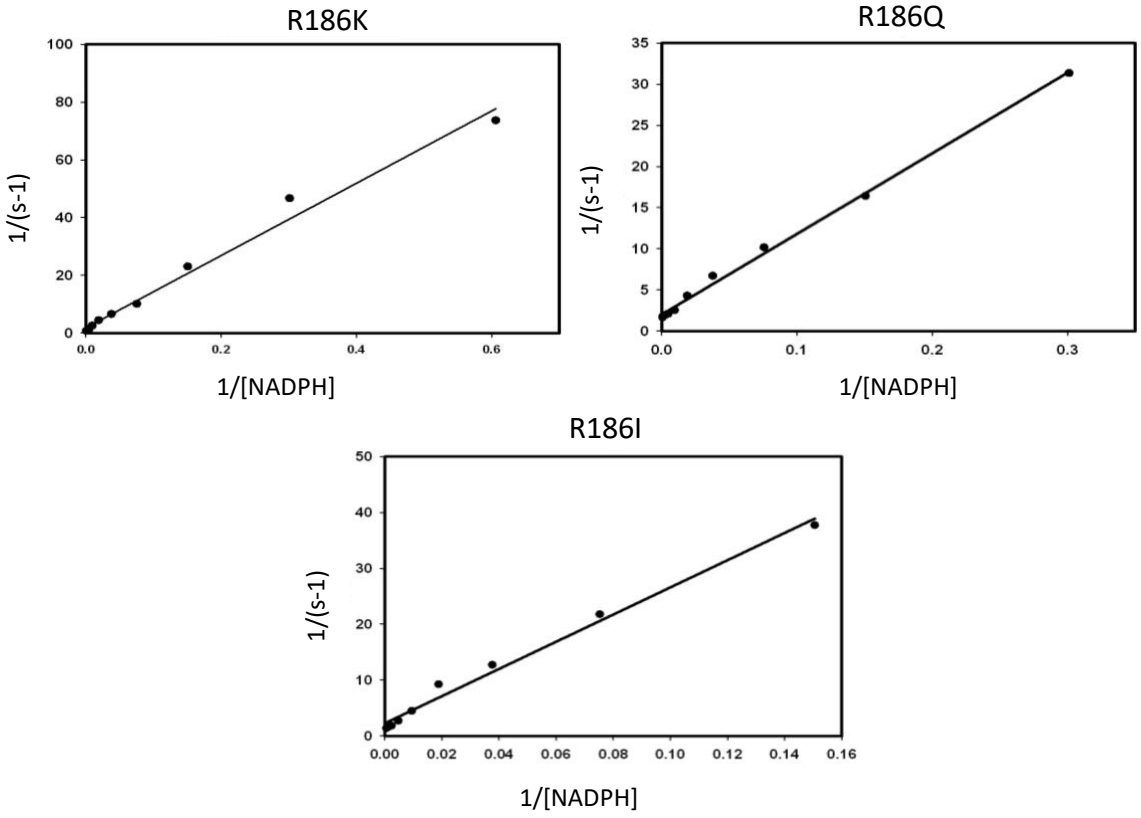

Figure 9. R186 Fno Variants double-reciprocal plots

The steady-state plots of T192A and T192V Fno variants displayed a curve downward and concave in curvature, like *wt*Fno (Figure 10). This contradicts what the Hill coefficients of the data implies. Future work will be to conduct the binding experiments again.

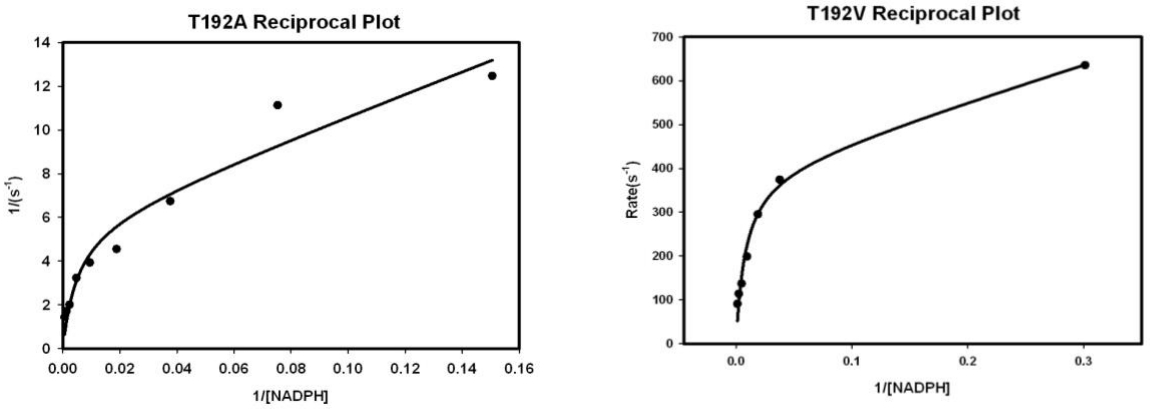

Figure 10. T192 Fno Variants double-reciprocal plots

Pre steady-state kinetic data

The pre steady-state experiments for the Fno variants were conducted under the same conditions as *wt*Fno (6). Like *wt*Fno, the spectra collected at different time intervals within the wavelength range of 350–800 nm did not show any formation of new peaks during the reaction, suggesting the absence of any observable intermediates. The reduction of the FO peak was monitored by absorbance changes at 420 nm. For each of the variants below, the reaction progress curve exhibited initial burst kinetics, followed by a slow phase rate. Unlike *wt*Fno, the fast phase rate is similar to the steady-state k_{cat}. This suggest that hydride transfer is rate-limiting in catalysis. The data revealed that within error, each of the mutations on residue R186 had similar fast phases as well slow phases, however each of these variants (R186K, R186Q and R186I) are significantly slower than that of *wt*Fno. T192A Fno is even slower that the R186 variants of Fno. As in *wt*Fno the magnitude of the burst phase corresponds to the amount of FO reduced by NADPH. For these variants the amount of production formation ranges from 54-63% (Table 4) and within error all of the R186 Fno mutations are the same (see appendix for plots).

Table 4: Pre Steady State-Kinetic Parameters for *wt*Fno and Variants

Pre-steady state kinetics parameters of *wt*Fno and variants. The rapid kinetic experiments were performed in the Hitech Scientific DX2 stopped-flow spectrophotometer at 22 °C. Fno (1.0, 1.5 and 2.0 μM; 50 mM MES/NaOH, pH 6.5, respectively) was mixed with 10 μM NADPH, forming the Fno-NADPH complex. FO (25 μM) in 50 mM MES/NaOH, pH 6.5 was then mixed with the Fno-NADPH complex.

Fno	Fast phase (s^{-1})	Slow phase (s^{-1})	Half Site Reactivity (%)
*wt*Fno	87 ± 2	1.99 ± 0.02	54 ± 1
R186K	1.7 ± 0.5	0.267 ± 0.002	63 ± 1
R186Q	1.3 ± 0.2	0.175 ± 0.001	62 ± 1
R186I	1.7 ± 0.3	0.368 ± 0.001	61 ± 1
T192A	0.7 ± 0.2	0.062 ± 0.004	54 ± 1

2.3 Conclusions

Our previous work suggest that Fno is a regulatory enzyme that produces NADPH within methanogenic organisms, as well as sulfate reducing organisms (6). *wt*Fno, displayed negative cooperativity kinetics, along with half-site reactivity, which means that when one subunit is active, the other subunit is not. The phenomena has lead to our next question, which was, how are the two subunits communicating with one another? We have previously identified several amino acids at the interface of the two subunits that likely affected inter-subunit communication (Figure 8). These amino acids are R186, T192, S190 and H133. Here, we examined the effects of R186, T192, S190, H133 residues on the inter-subunit communication within Fno using binding studies, steady-state and pre steady-state kinetic methods. The conversion of R186 to a lysine, glutamine and isoleucine decreased the large charge of the guanidium group to a small charge and then no charge with the polarity kept intact. Once the arginine was converted to an isoleucine, the side chain was converted to a nonpolar molecule with no charge. The conversion of T192 to an alanine and valine took away the polarity of this amino acid as

well as affecting the size. The conversion of S190 to an alanine took away all polarity. In the conversion of histidine to asparagine, the aromaticity was removed, while the polarity was maintained. Our results were compared to *wt*Fno, which was previously reported (6).

Our binding studies suggest that R186 have a Hill Coefficient of about 1, suggesting no cooperativity for NADPH. R186I has a Hill Coefficient of less than 1, suggesting negative cooperativity for this variant. *wt*Fno, displays negative cooperativity, similar to some of the R186 variants. However, for the R186K and R186Q Fno variants, this cooperativity or inter-subunit communication has changed.

The steady-state kinetic analysis of R186I and T192V Fno variants are inconsistent with the Hill coefficient values that are displayed during the binding experiments. The double reciprocal of the T192V variant with respect to NADPH displays a downward and concave curvature which is indicative of negative cooperativity, while the double reciprocal of the R186 Fno variant with respect to NADPH does not (Figures 9 - 10).

The pre steady-state data with F_{420} cofactor and NADPH for the Fno variants revealed biphasic kinetics with a fast and slow phase, similar to what was seen previously with *wt*Fno. For each of the variants, the reaction progress curve exhibited initial burst kinetics, followed by a slow phase rate. The data revealed that hydride transfer is rate-limiting within these variants.

In summary, our data suggests that all of the amino acids are important in catalysis. More importantly, R186 and T192 are vital to inter-subunit communication. When these amino-acids are converted to something else, communication is disrupted and cooperativity kinetics is no longer displayed.

Appendix

Binding Isotherms

Fig. A-1-1

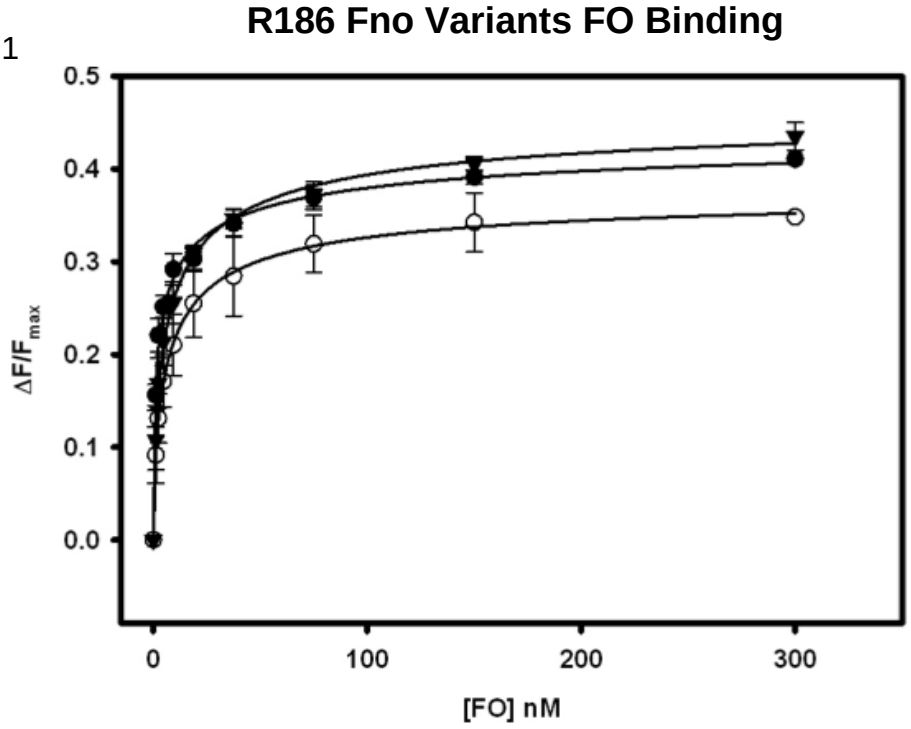

Fig. A-1-2

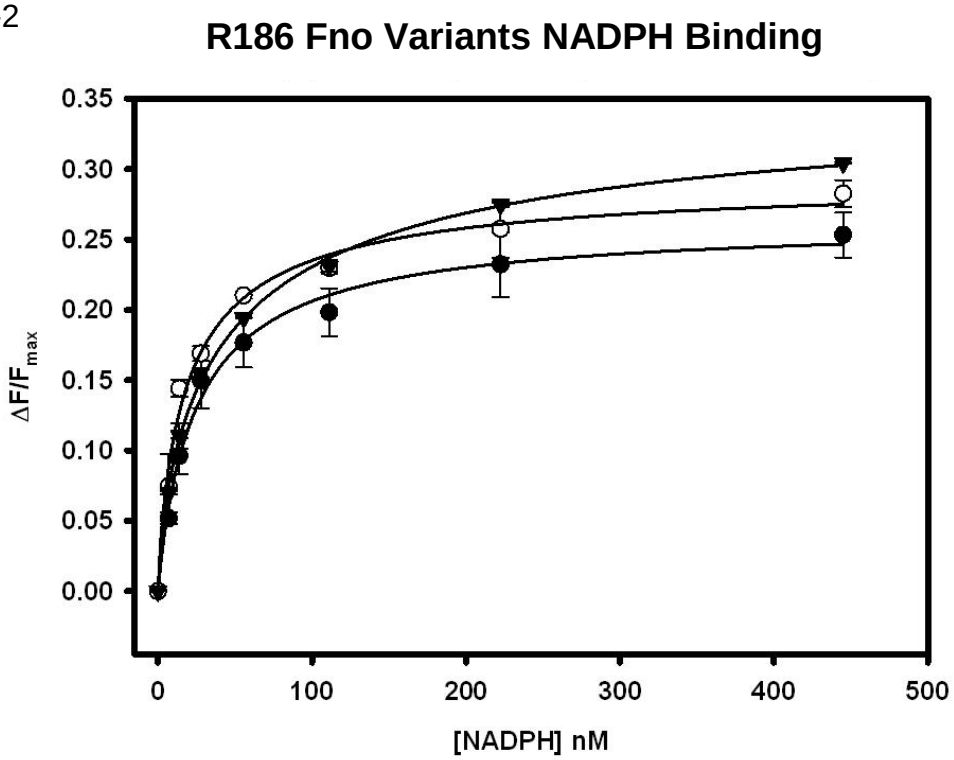

Fig. A-1-3

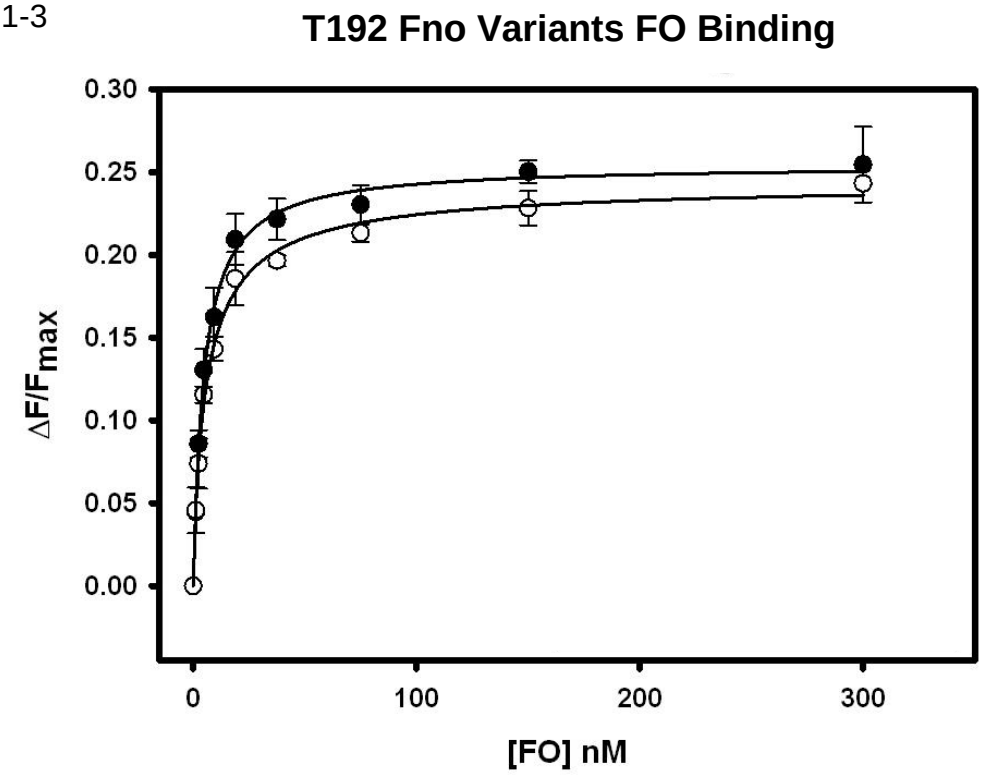

Fig. A-1-4

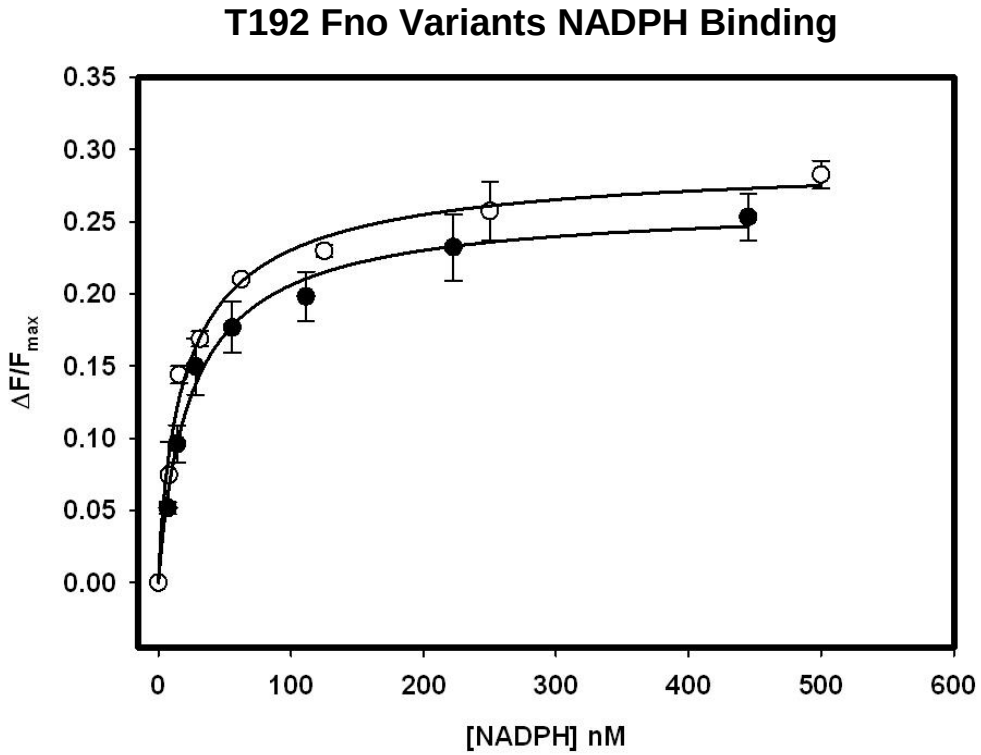

Fig. A-1-5

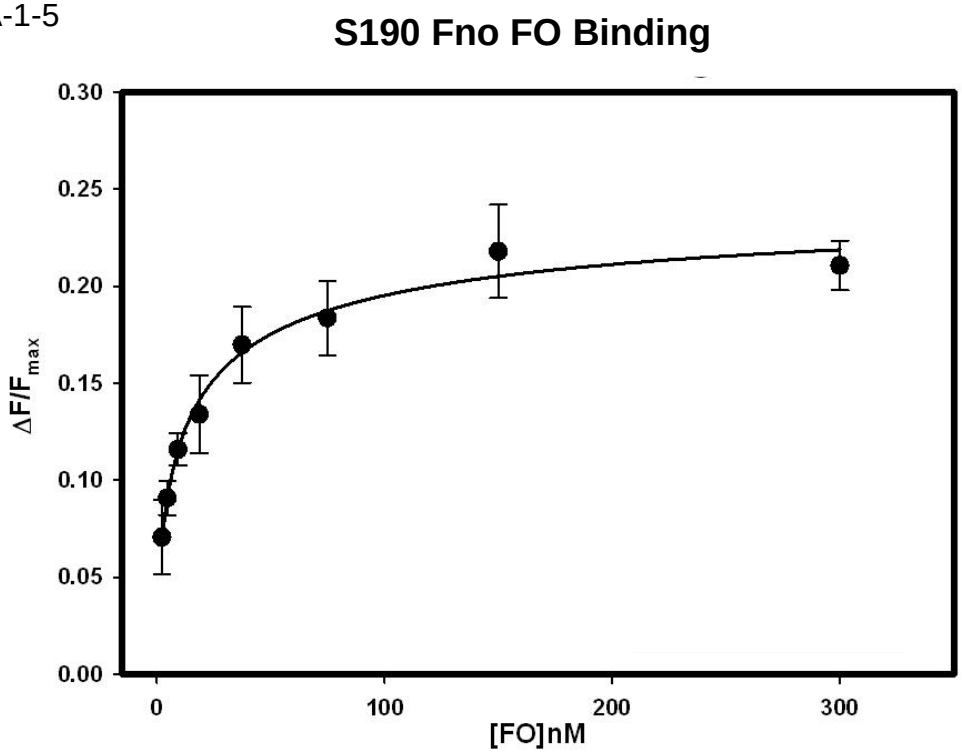

Fig. A-1-6

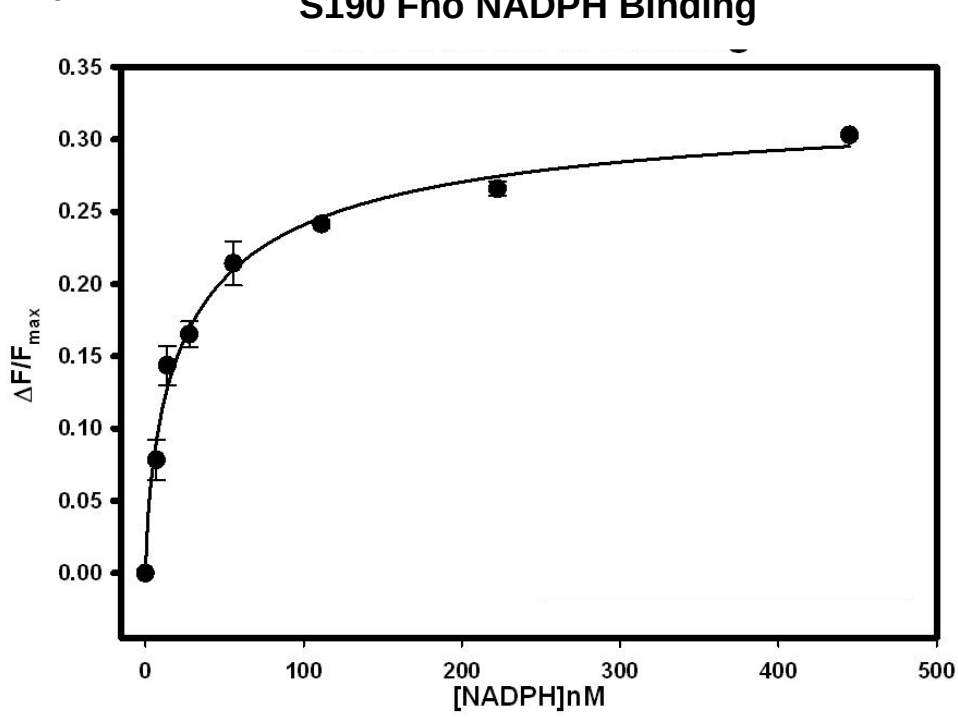

Fig. A-1-7

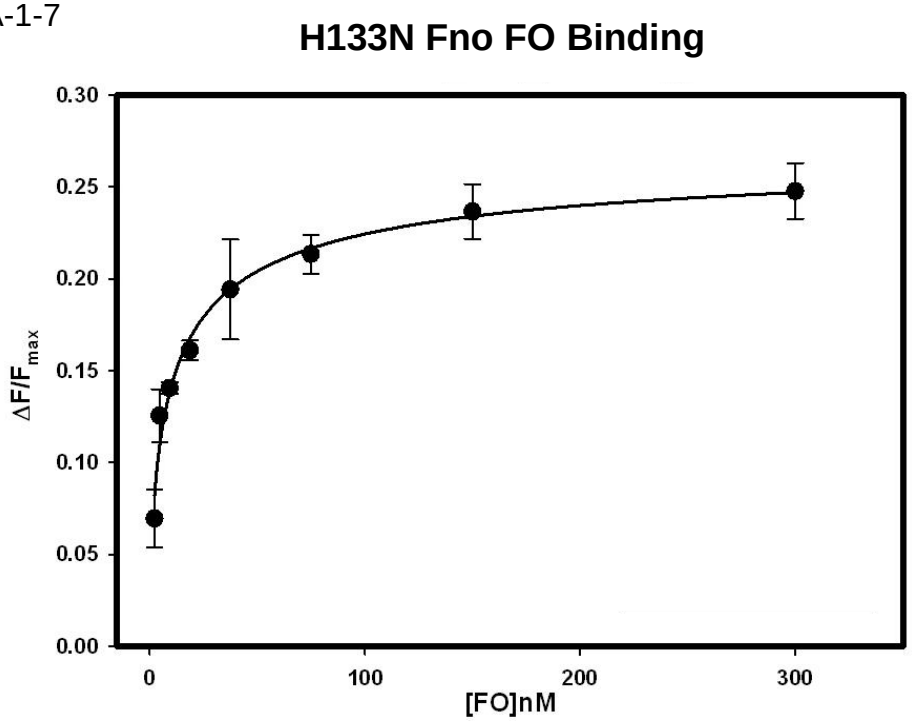

Fig. A-1-8

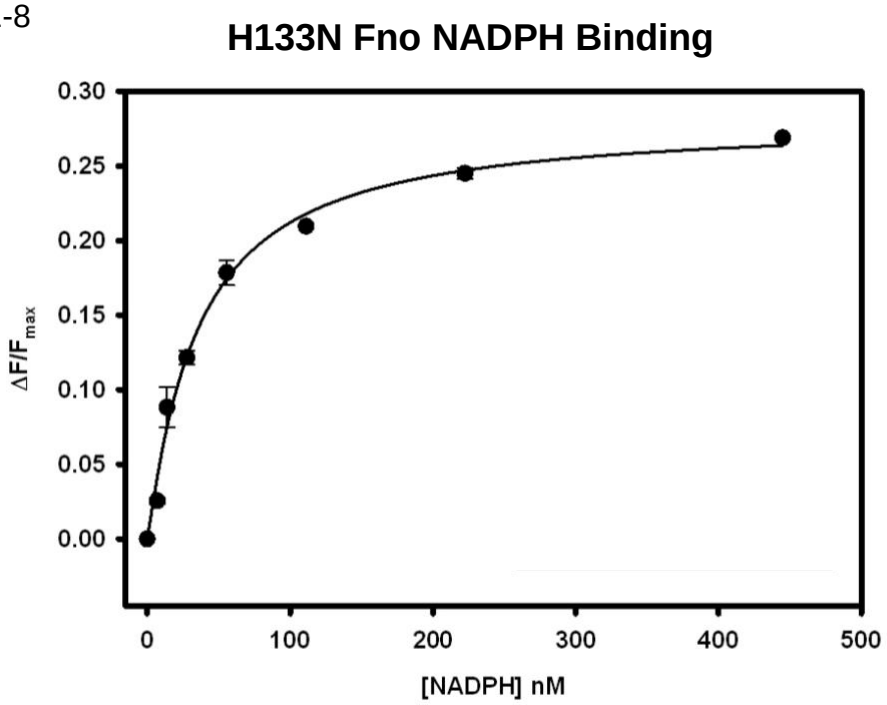

Steady-state Kinetics

Fig. A-2-1 **R186K Fno NADPH Steady-State**

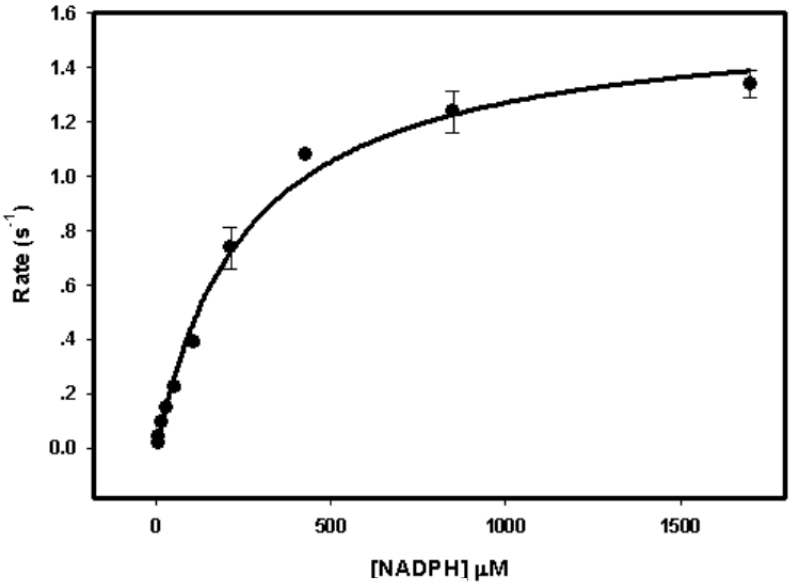

Fig. A-2-2 **R186K Fno FO Steady-State**

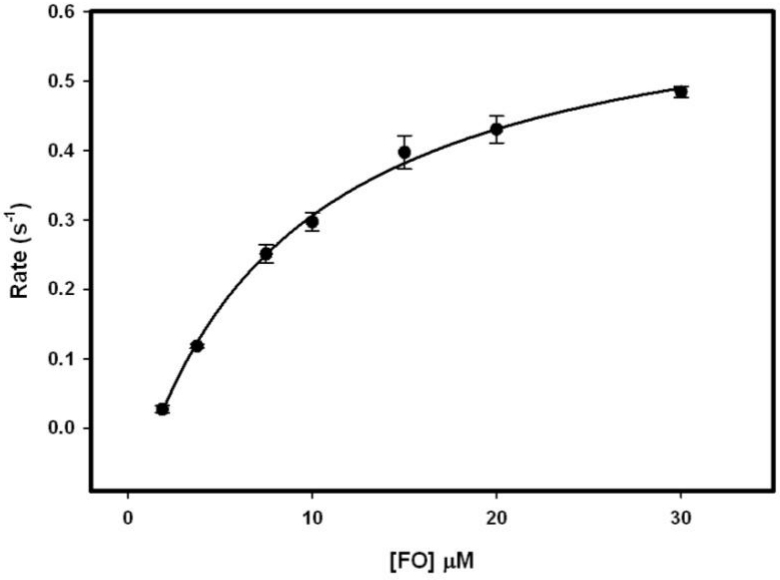

Fig. A-2-3

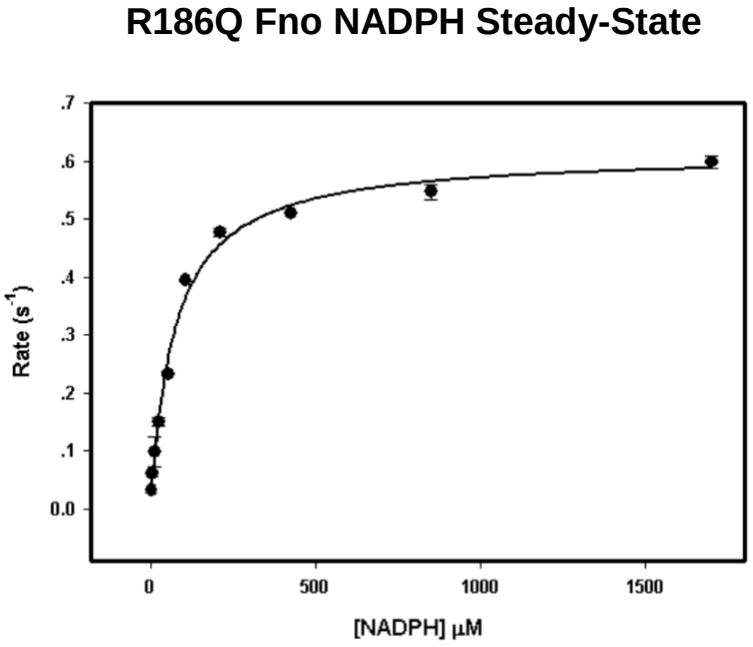

Fig. A-2-4

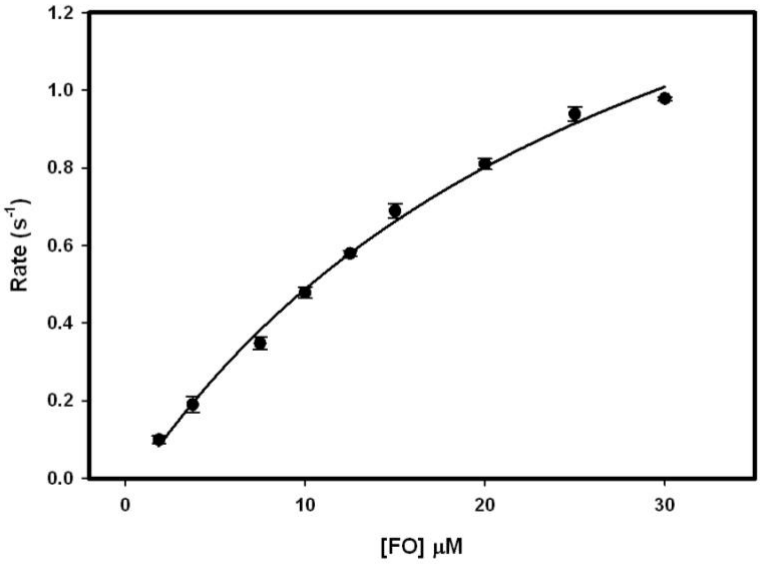

Fig. A-2-5

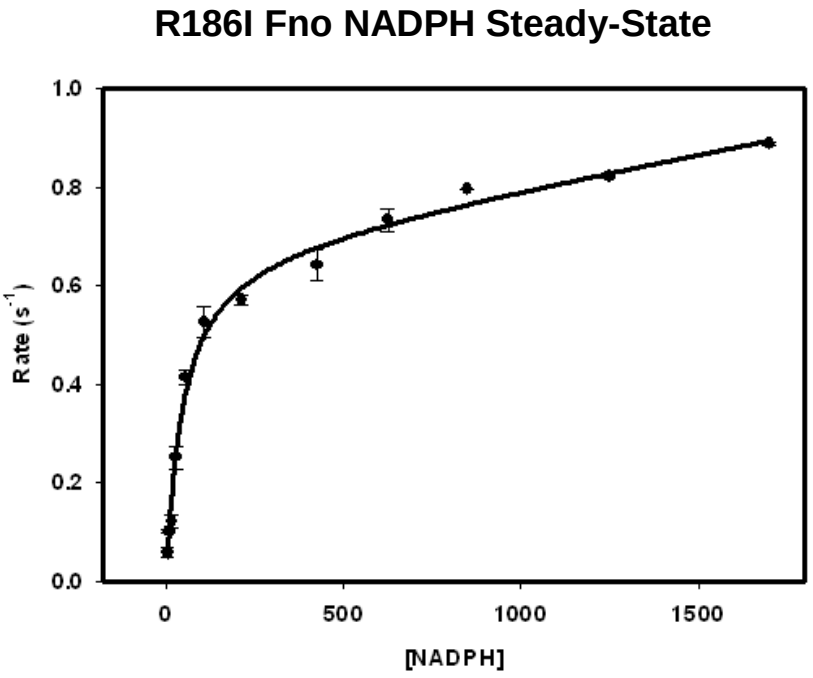

Fig. A-2-6

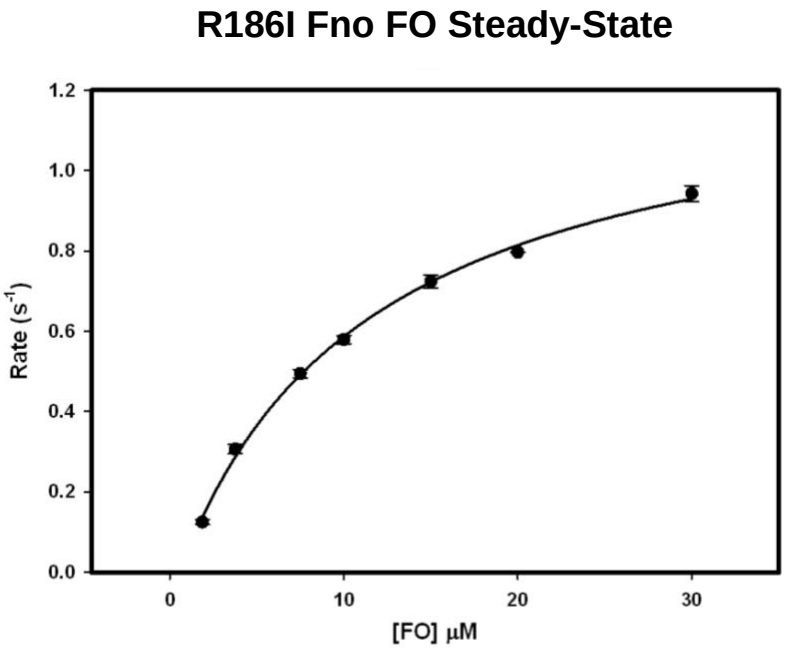

Fig. A-2-7

T192A Fno NADPH Steady-State

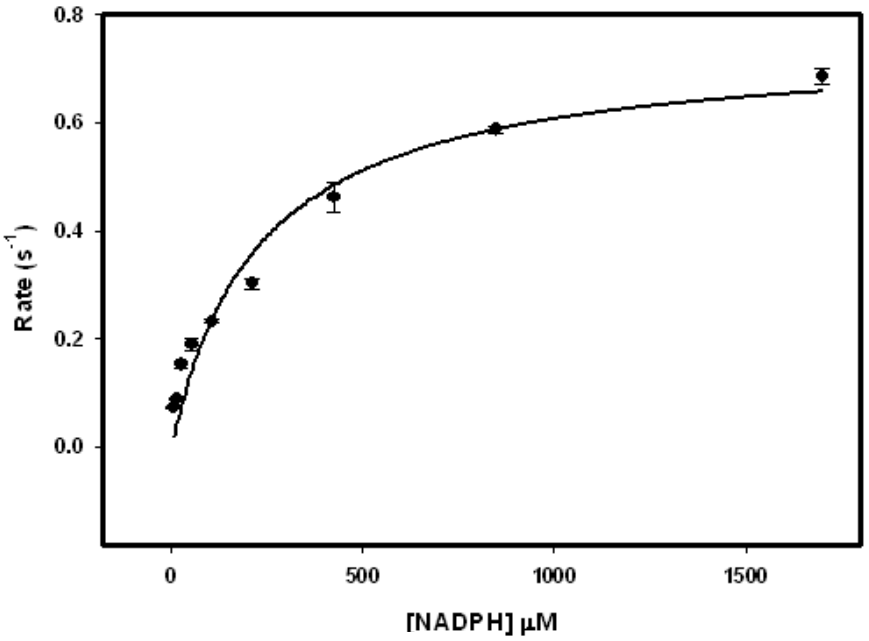

Fig. A-2-8

T192A Fno FO Steady-State

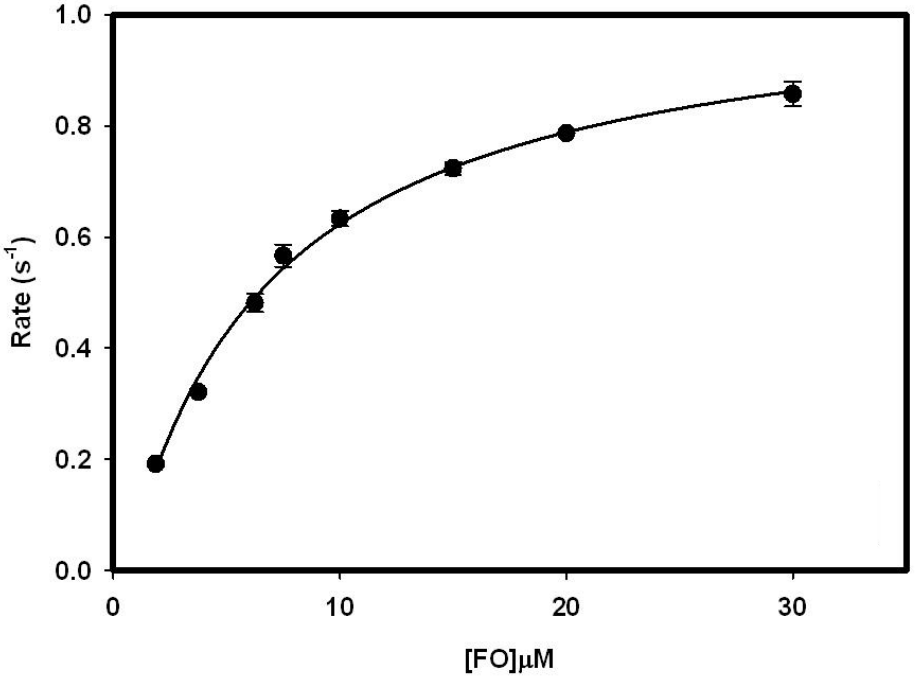

Fig. A-2-9

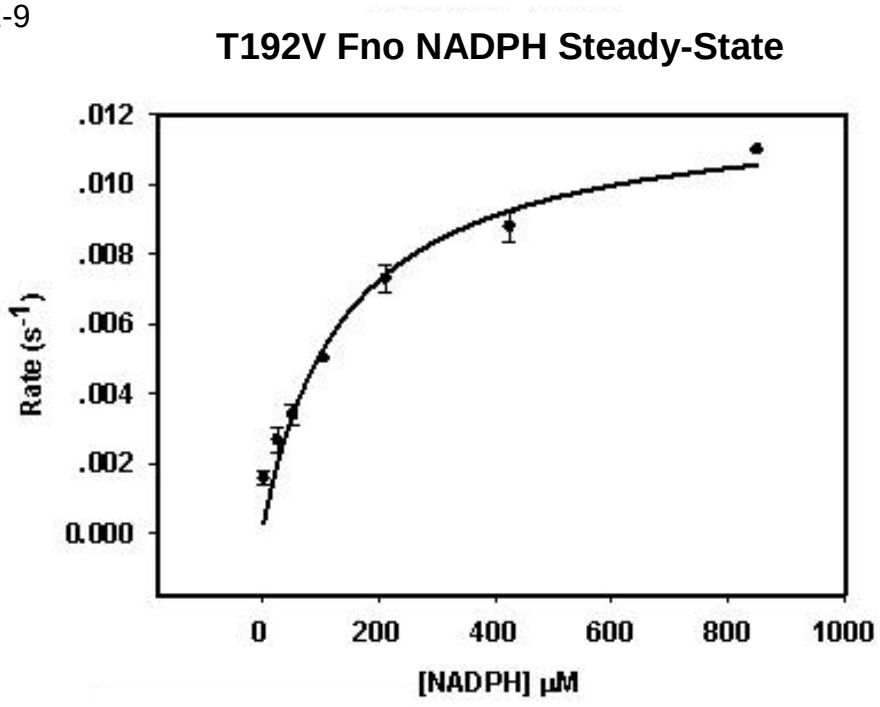

Fig. A-2-10

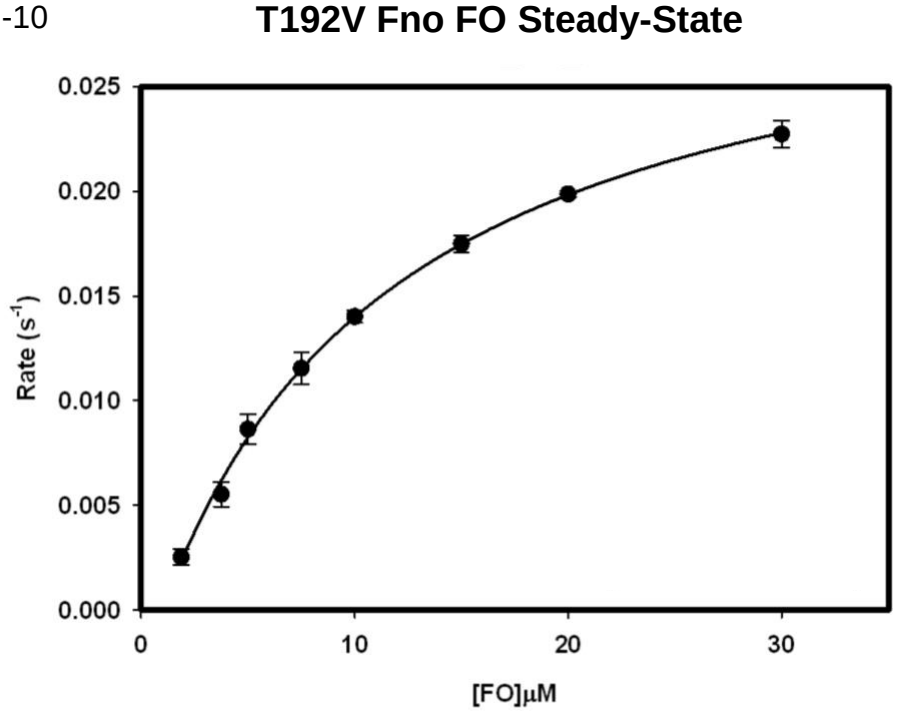

Pre steady-state

Fig. A-3-1

R186K Fno 2 μM Pre Steady-State

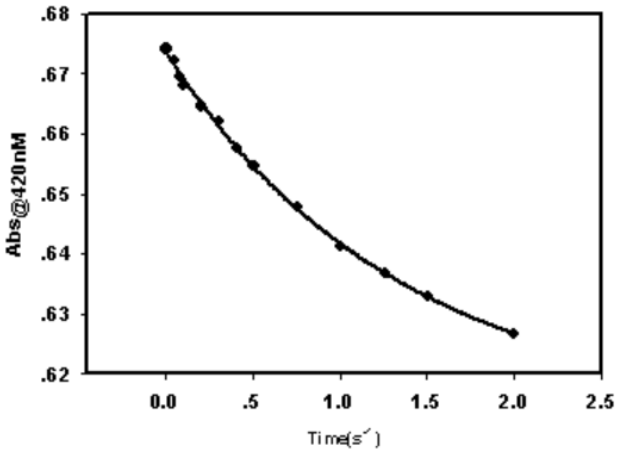

Fig. A-3-2

R186K Fno 1.5 μM Pre Steady-State

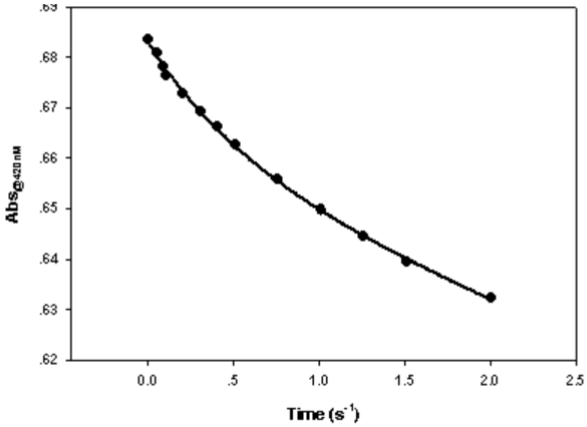

Fig. A-3-3

R186K Fno 1 μM Pre Steady-State

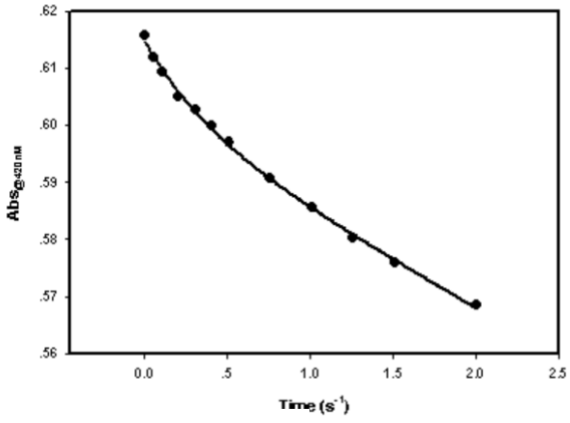

Fig. A-3-4

R186Q Fno 2 μM Pre Steady-State

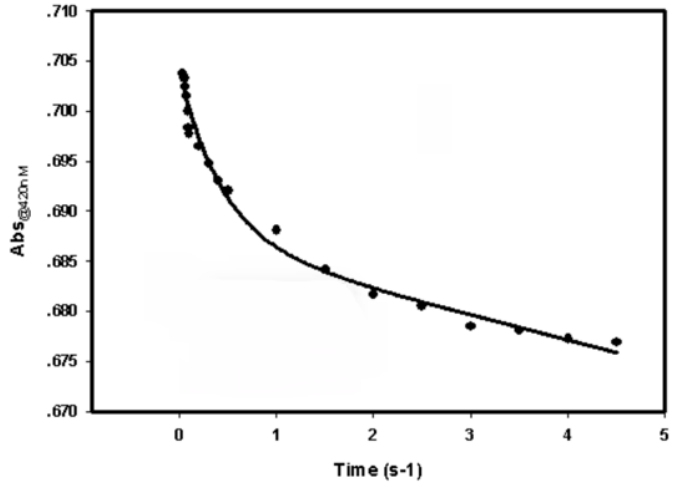

Fig. A-3-5

R186Q Fno 1.5 μM Pre Steady-State

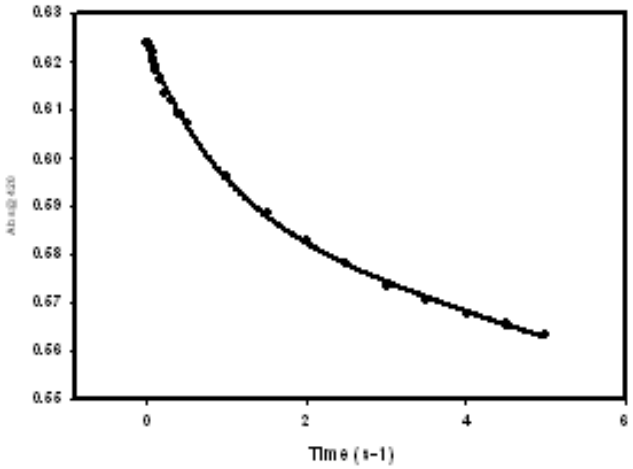

Fig. A-3-6

R186Q Fno 1 μM Pre Steady-State

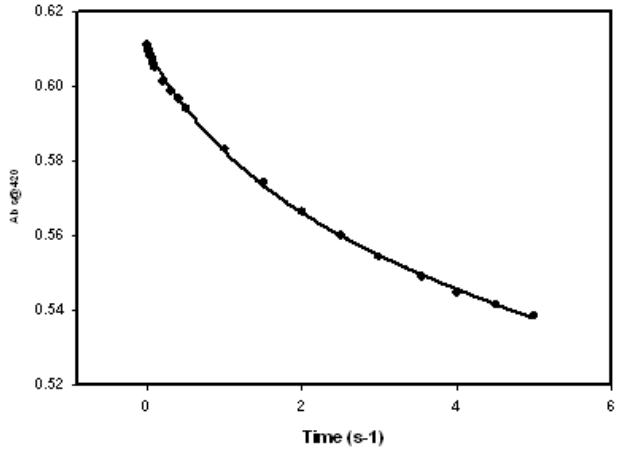

Fig. A-3-7

R186I Fno 2 μM Pre Steady-State

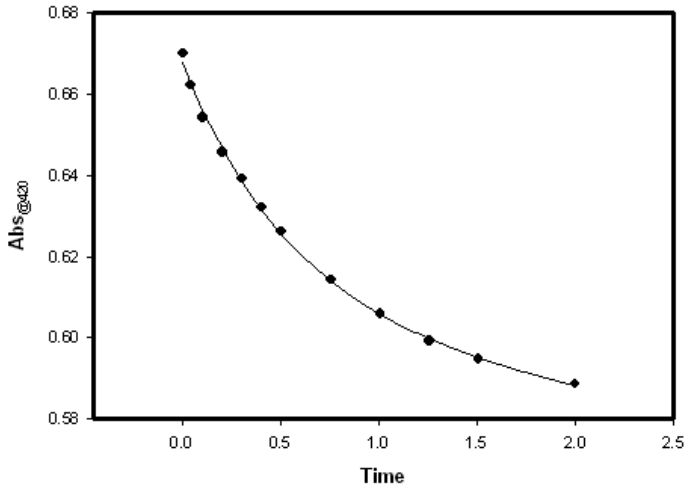

Fig. A-3-8

R186I Fno 1.5 μM Pre Steady-State

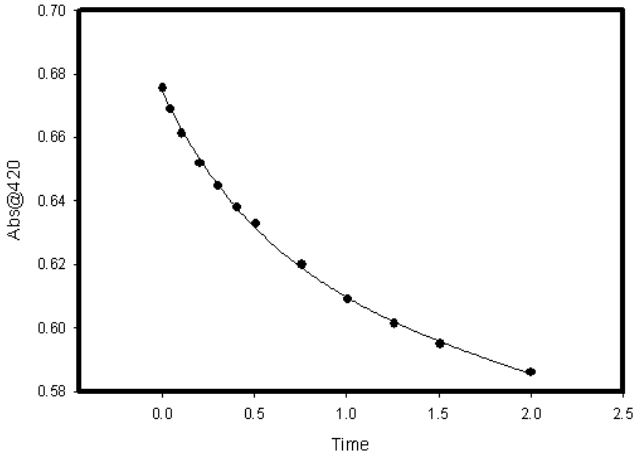

Fig. A-3-9

R186I Fno 1 μM Pre Steady-State

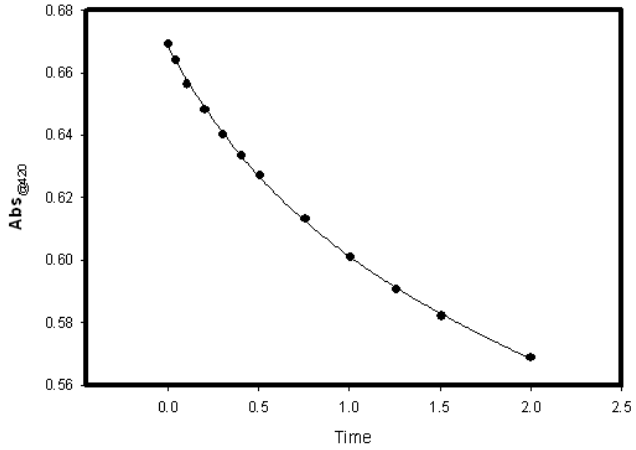

T192A Fno 2 μM Pre Steady-State

Fig. A-3-10

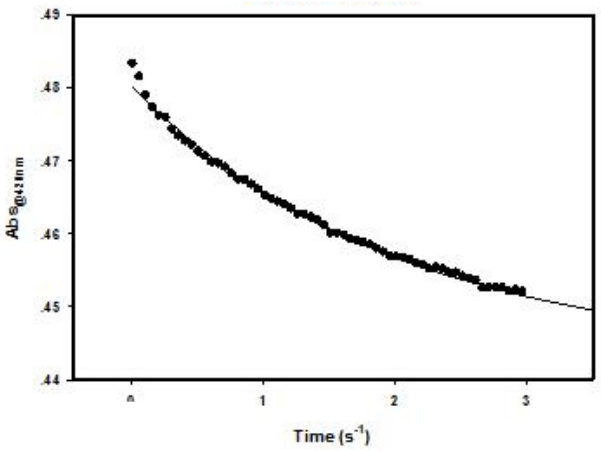

Fig. A-3-11

T192A Fno 1.5 μM Pre Steady-State

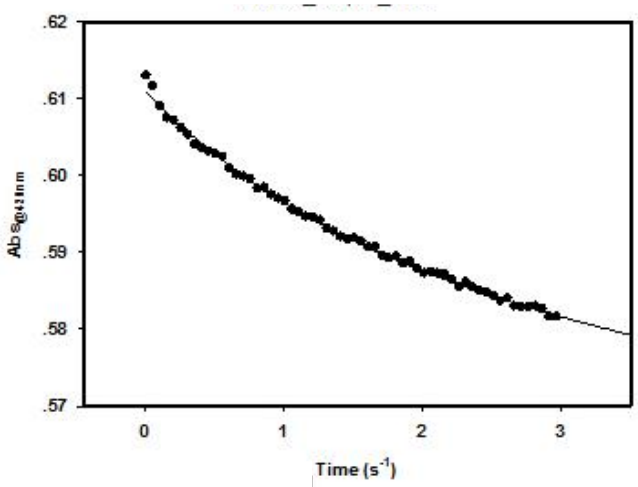

Fig. A-3-12

T192A Fno 1 μM Pre Steady-State

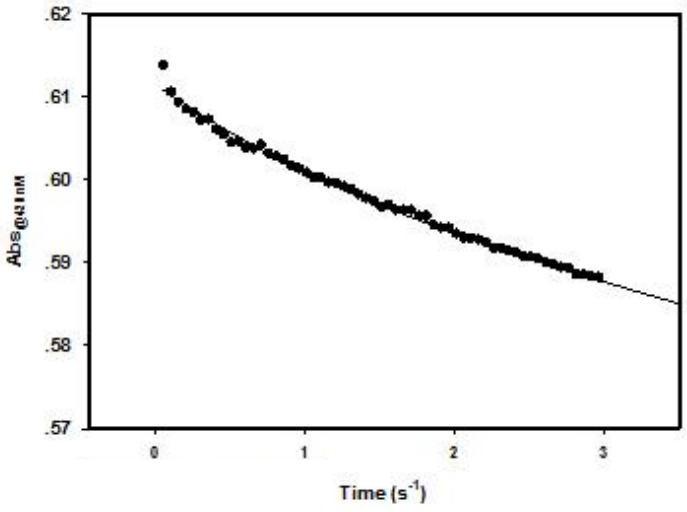

References

1. Warkentin, E., Mamat, B., Sordel-Klippert, M., Wicke, M., Thauer, R. K., Iwata, M., Iwata, S., Ermler, U., and Shima, S. (2001) Structures of F420H2:NADP+ oxidoreductase with and without its substrates bound. EMBO J. 20, 6561−6569.

2. Elias, D. A., Juck, D. F., Berry, K. A., & Sparling, R. Purification of the NADP(+):F(420) oxidoreductase of methanosphaera stadtmanae. *Can J Microbiol.* (2000)*, 46*(11), 998-1003.

3. Levitzki A, Koshland DE Jr. Negative cooperativity in regulatory enzymes. *Proc Natl Acad Sci U S A*. 1969;62(4):1121–1128. doi:10.1073/pnas.62.4.1121

4. Ersahin ME, Gomec CY, Dereli RK, Arikan O, Ozturk I. Biomethane production as an alternative bioenergy source from codigesters treating municipal sludge and organic fraction of municipal solid wastes. *J Biomed Biotechnol*. 2010;2011:953065. doi:10.1155/2011/953065

5. Cheeseman P, Toms-Wood A, Wolfe RS. Isolation and properties of a fluorescent compound, factor 420 , from Methanobacterium strain M.o.H. *J Bacteriol*. 1972;112(1):527–531.

6. Joseph E., Ebenezer Joseph, Cuong Quang Le, Toan Nguyen, Mercy Oyugi, Mohammad Shawkat Hossain, Frank W. FossJr., and Kayunta Johnson-Winters, Evidence of Negative Cooperativity nd Half-Site Reactivity within an F420-Dependent Enzyme: Kinetic Analysis of F420H2:NADP( ) Oxidoreductase. Biochemistry (Easton). 2 0;55:1082-90.

7 Greening C, Ahmed FH, Mohamed AE, et al. Physiology, Biochemistry, and Applications of F420- and Fo-Dependent Redox Reactions. *Microbiol Mol Biol Rev*. 2016;80(2):451–493. Published 2016 Apr 27. doi:10.1128/MMBR.00070-15

8. Edwards T, McBride BC. New method for the isolation and identification of methanogenic bacteria. *Appl Microbiol*. 1975;29(4):540–545.

9. Doddema HJ, Vogels GD. Improved identification of methanogenic bacteria by fluorescence microscopy. *Appl Environ Microbiol*. 1978;36(5):752–754.

10. van Beelen, P., Dijkstra, A.C. & Vogels, G.D. Quantitation of coenzyme F420 in methanogenic sludge by the use of reversed-phase high-performance liquid chromatography and a fluorescence detector. Eur J Appl Microb Biotechnol. 1983;18(1):67-9.

11. Dolfing J, Mulder JW. Comparison of methane production rate and coenzyme f(420) content of methanogenic consortia in anaerobic granular sludge. *Appl Environ Microbiol*. 1985;49(5):1142–1145.

12. Reynolds PJ, Colleran E. Evaluation and improvement of methods for coenzyme F420 analysis in anaerobic sludges. Journal of Microbiological Methods. 1987;7(2):115-30.

13. Ashby KD, Casey TA, Rasmussen MA, Petrich JW, Steady-state and time-resolved spectroscopy of F420 extracted from methanogen cells and its utility as a marker for fecal contamination. J Agric Food Chem. 3 0;49(3):1123-7.

14 Yong Sung Kim, Maria Westerholm, Paul Scherer, Dual investigation of methanogenic processes by quantitative PCR and quantitative microscopic fingerprinting, *FEMS Microbiology Letters*, Volume 360,(2014): 76–84

15 Patiño S, Alamo L, Cimino M, Casart Y, Bartoli F, García MJ, Salazar L. Autofluorescence of mycobacteria as a tool for detection of Mycobacterium tuberculosis. *J Clin Microbiol*. 2008 Oct;46(10):3296-302. doi: 10.1128/JCM.02183-08. Epub 2008 Jun 25. PubMed PMID: 18836064; PubMed Central PMCID: PMC2566091.

16. Maglica Ž, Özdemir E, McKinney JD. Single-cell tracking reveals antibiotic-induced changes in mycobacterial energy metabolism. *MBio*. 2015;6(1):e02236-14. Published 2015 Feb 17. doi:10.1128/mBio.02236-14

17. Anthony A. DiMarco, Thomas A. Bobik, and Ralph S. Wolfe. Unusual coenzymes of methanogenesis. Annu Rev Biochem. 1990;59(1):355-94.

18 Berk, Holger and Thauer, Rudolf K.(1998), $F_{420}H_2$:NADP oxidoreductase from *Methanobacterium thermoautotrophicum*: identification of the encoding gene via functional overexpression in *Escherichia coli* , *FEBS Letters*, 438, doi: 10.1016/S0014-5793(98)01288-5

19. Jacobson, F., and Walsh, C. (1984) Properties of 7,8-didemethyl- 8-hydroxy-5-deazaflavins relevant to redox coenzyme function in methanogen metabolism. Biochemistry 23, 979−988.

20 Arora K, Brooks Iii CL 3rd. Functionally important conformations of the Met20 loop in dihydrofolate reductase are populated by rapid thermal fluctuations. *J Am Chem Soc*. 2009;131(15):5642–5647. doi:10.1021/ja9000135

21. Stojković V, Perissinotti LL, Lee J, Benkovic SJ, Kohen A. The effect of active-site isoleucine to alanine mutation on the DHFR catalyzed hydride-transfer. *Chem Commun (Camb)*. 2010;46(47):8974–8976. doi:10.1039/c0cc02988b

22. Kohen A, Klinman JP. Hydrogen tunneling in biology. (1999) Chem Biol. 7 0;6(7):191.

23. de Wit, L. E. A., Eker APM. 8-Hydroxy-5-deazaflavin-dependent electron transfer in the extreme halophile Halobacterium cutirubrum. FEMS Microbiology Letters. 1987;48(1):121-5.

24. Nest KE. Cooperativity in enzyme function: Equilibrium and kinetic aspects. Methods Enzymol. 1995;249:519-67.

25. Hossain, M. S., Le, C. Q., Joseph, E., Nguyen, T. Q., Johnson- Winters, K., and Foss, F. W., Jr. (2015) Convenient synthesis of deazaflavin cofactor FO and its activity in F420-dependent NADP reductase. Org. Biomol. Chem. 13, 5082−5085.

26. Le CQ, Oyugi M, Joseph E, Nguyen T, Ullah MH, Aubert J, Phan T, Tran J, Johnson-Winters K. Effects of isoleucine 135 side chain length on the cofactor donor-acceptor distance within $F_{420}H_2$:$NADP^+$ oxidoreductase: A kinetic analysis. *Biochem Biophys Rep*. 2016 Nov 30;9:114-120. doi: 10.1016/j.bbrep.2016.11.012. PubMed PMID: 28955995; PubMed Central PMCID: PMC5614548.